

NATURE AND ORIGIN OF MINERAL COATINGS ON VOLCANIC ROCKS
OF THE BLACK MOUNTAIN, STONEWALL MOUNTAIN, AND KANE
SPRINGS WASH VOLCANIC CENTERS, SOUTHERN NEVADA

Dr. James V. Taranik, Principal Investigator
Dr. Donald C. Noble, Co-Principal Investigator
Dr. Liang C. Hsu, Co-Investigator
David M. Spatz, Co-Investigator

Mackay School of Mines
Department of Geological Sciences
University of Nevada, Reno
Reno, Nevada 89557

January, 1987
Semiannual Progress Report for Period July, 1986 -
January, 1987

Contract Number NAS5-28765 ✓

(NASA-CR-180183) NATURE AND ORIGIN OF
MINERAL COATINGS ON VOLCANIC ROCKS OF THE
BLACK MOUNTAIN, STONEWALL MOUNTAIN, AND KANE
SPRINGS, WASH VOLCANIC CENTERS, SOUTHERN
NEVADA Semiannual Progress Report, Jul.

N87-18255

Unclas
G3/46 43349

Prepared for
The National Aeronautics and Space Administration
Goddard Space Flight Center
Greenbelt, Maryland 20771

CONTENTS

	Page
Abstract	1
Introduction	2
Study Sites	2
Method of Investigation	7
Data acquisition	7
Field investigation	10
Imagery processing	10
Laboratory research	17
General Imagery Applications	19
Coating in Desert Environments	23
Geologic Setting	26
Stonewall Mountain	26
Black Mountain	30
Kane Springs	34
Individual Volcanic Units	36
Stonewall Mountain	36
Black Mountain	38
Kane Springs	40
Imagery Characteristics	43
Stonewall Mountain	43
Black Mountain	50
Kane Springs	54
Coatings	57
Conclusions	60
References	62

FIGURES

	Page
1 General Location Map	3
2 Kane Springs Topo	4
3 Stonewall & Black Mountain topo	5
4 Location Landsat Scenes	8
5 Sample Locations - Stonewall	11
6 Sample Locations - Black Mountain	12
7 Sample Locations - Kane Springs	13
8 Landsat Platform & Communications Link	20
9 Thematic Mapper Characteristics	21
10 Volcanic Centers of Nevada	27
11 Geologic Map - Stonewall	28
12 Geologic Map - Black Mountain	31
13 Geologic Map - Kane Springs	35
14 Composite Image - Stonewall	49
15 Composite PC Image - Stonewall	49
16 Composite ISH Image - Black Mountain	51
17 Composite Image - Kane Springs	51
18 Photomicrograph, Coatings	58
19 Photomicrograph, Rind & Coatings	58

TABLES

1 List of Landsat Data Acquired	9
2 List of Data Processing Equipment	14
3 Volcanic Events at Black Mountain	33
4 Statistical Data - Stonewall	44
5 Statistical Data - Black Mountain	45
6 Statistical Data - Kane Springs	46
7 Principle Components Statistics	47

ABSTRACT

Landsat Thematic Mapper imagery was evaluated over 3 Tertiary calderas in southern Nevada. Each volcanic center derived from a highly evolved silicic magmatic system represented today by well exposed diverse lithologies. Distinctive imagery contrast between some of the late ash flows and earlier units follows from the high relative reflectance in longer wavelength bands (bands 5 and 7) of the former. Enhancement techniques involving band ratioing, ISH transform, principle components analysis, and hybrid combinations of hue, saturation, and PC's with non-redundant individual bands and band ratios, provide color composite images which highlight some of the units in remarkable color contrast. Some of these units were previously unmapped.

Inasmuch as coatings on the tuffs are incompletely developed and apparently largely dependent spectrally on rock properties independent of petrochemistry, such as degree of welding, vapor phase alteration, and hyalinity; and vegetative cover sparse - 20-30% over these units - it is felt that the distinctive imagery characteristics is more a function of primary lithologic or petrochemical properties. Any given outcrop is backdrop for a variety of cover types, of which coatings, at various stages of maturity, are one.

Petrographic and X-ray diffraction analysis of the outer air-interface zone of coatings reveals they are composed chiefly of amorphous compounds, probably with varying proportions of iron and manganese. Coatings are extremely thin - less than 0.1mm thick - and in contact for the most part with apparently unaltered rock. Kaolinite was identified in coating samples from 2 lava flows, and illite from 2 tuffs. Clay minerals, however, do not appear to be an important coating component.

These observations, although preliminary, support an origin for some outer (air-interface) coating constituents exogenous to underlying host. Further analytical efforts, including XRF and SEM investigations, are continuing.

INTRODUCTION

In April, 1984, the Mackay School of Mines, University of Nevada, Reno was awarded a 3-year contract by NASA to investigate Landsat Thematic Mapper imagery over Tertiary volcanic centers in southern Nevada. Three silicic calderas were selected.

Reflected electromagnetic sensing techniques essentially measure surface cover. In the case of rock cover, surficial coatings resulting primarily from secondary weathering processes are detected. It was decided, therefore to focus this investigation on the nature and origin of coatings on the various volcanic rock assemblages at each site.

A five-phase investigative program was proposed: 1) an a priori imagery assessment by individuals familiar with processing techniques but without detailed knowledge of the geology at the sites under investigation (other than that they are caldera settings); 2) field investigations involving sampling of lithologies and coatings, notations on general observations, and ground based photography; 3) further imagery processing based on field experience and general mapping results; 4) laboratory analysis including thin section study of coatings, X-ray diffraction (XRD) analysis of coating mineralogy, X-ray fluorescence (XRF) analysis of host rock and coating compositions, scanning electron microscope (SEM) observations, and possibly microprobe studies; 5) final field correlation and verification.

First phase imagery processing was completed in the winter of 1986. Field sampling, observation, and ground based photography was completed during the summer, 1986. Second phase imagery evaluation and imagery mapping assessments were completed in the fall of 1986. Laboratory analysis is the current focus: over 50 thin sections have been studied to varying degrees of detail and fifty-two XRD analyses have been completed. Analytical work planned for this coming winter includes XRF and SEM analyses on coatings, whole rock, and weathering rinds.

STUDY SITES

The three study sites selected for investigation (Figures 1, 2, and 3) provide superior settings in

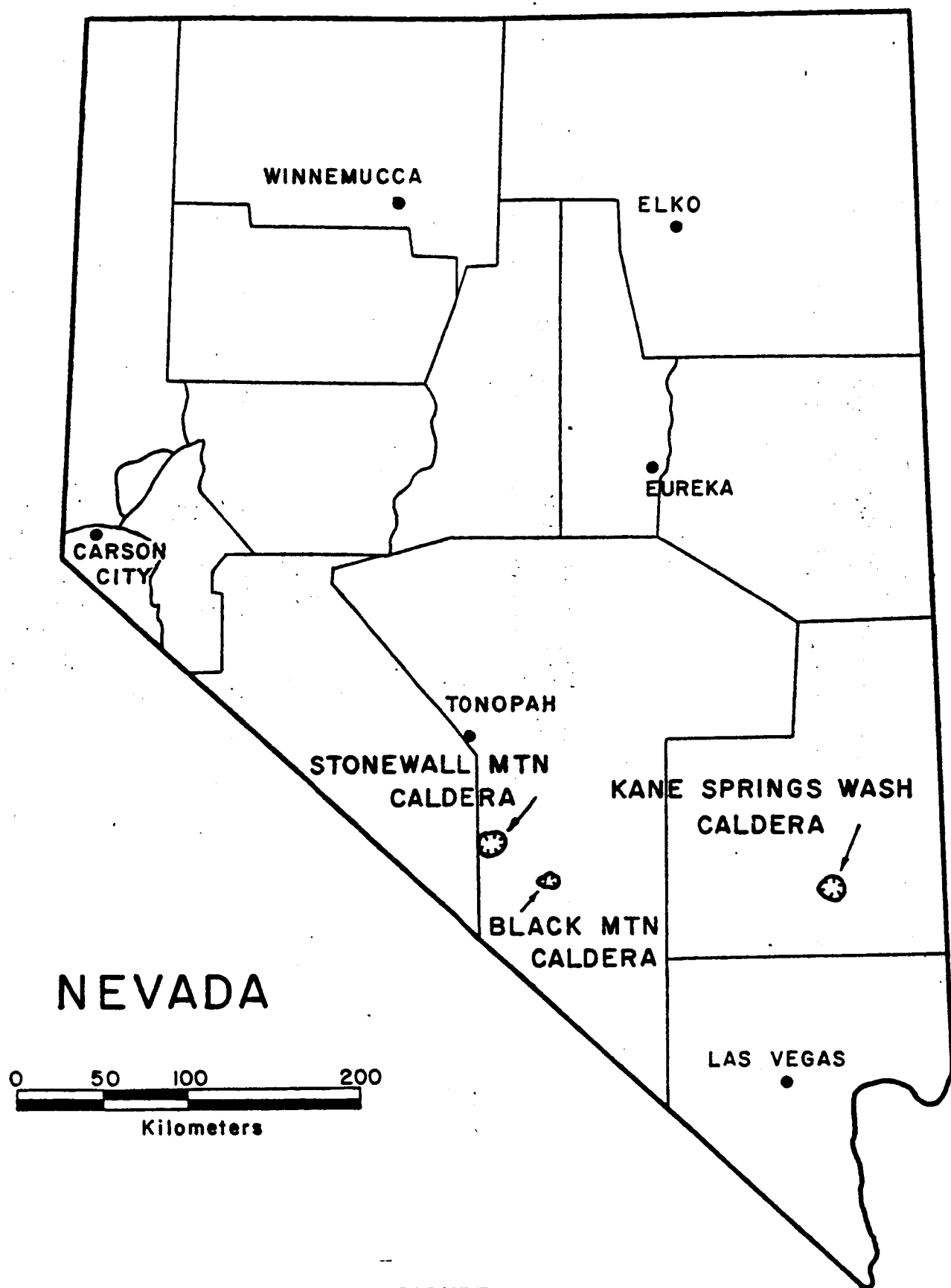


FIGURE 1
LOCATION OF LANDSAT TM TEST SITES

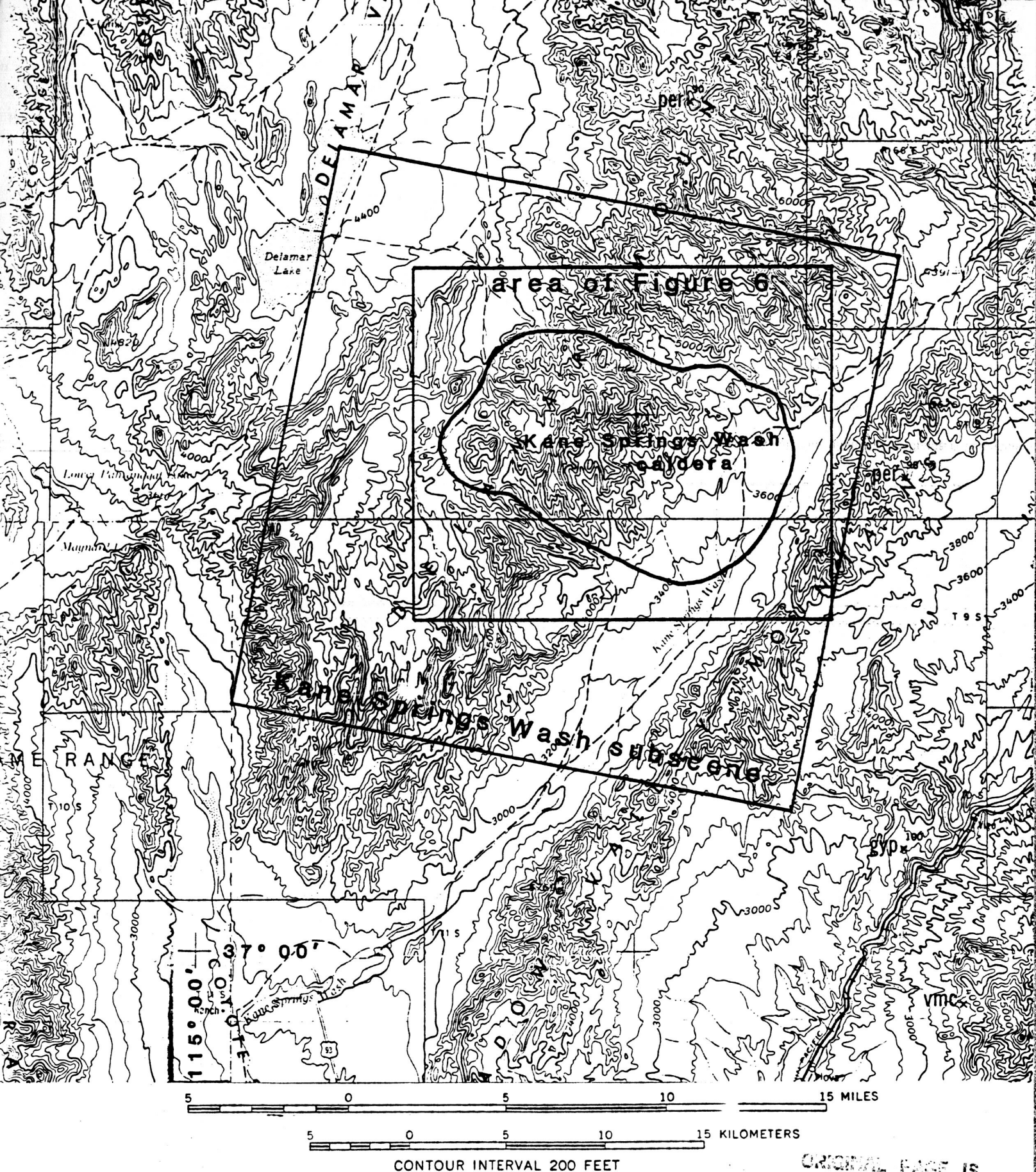


Figure 2 Topographic map of part of Lincoln, County, Nevada, showing locations of Kane Springs Wash subscene and figure 6 (from Tschanz and Pampeyan, 1972).

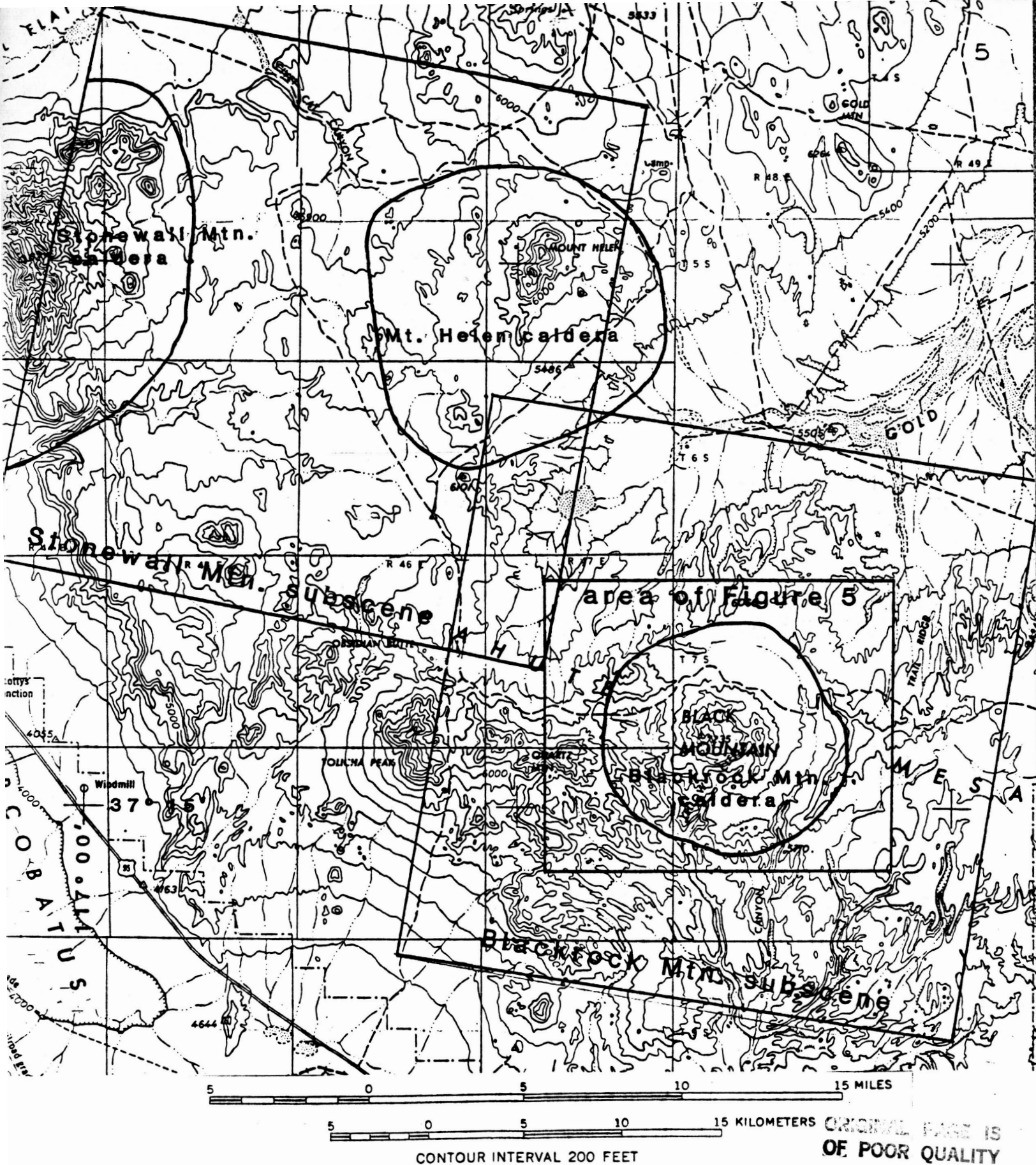


Figure 3. Topographic map of part of Nye County, Nevada, showing locations of Stonewall Mountain subscene, Blackrock Mountain subscene, and figure 5 (from Cornwall, 1972).

terms of exposure, preservation, diversity, and an already existing data base collected by previous researchers at Mackay. Each study site is approximately 9 x 9 miles (14.5 x 14.5 kilometers) and encompassed within a 512 x 512 pixel Landsat 5 TM subscene. Each site centers on or straddles a well defined youthful caldera structure with discrete ash flow tuff deposits and associated lavas and subvolcanic intrusive bodies. Each center was the source for multiple outflow sheets that extend from the calderas up to 30 km distally. Some of these major pyroclastic sheets are distinct chemically, mostly in regard to iron content, both divalent species as well as trivalent, resulting from auto-oxidation processes during deposition and cooling. Devitrification, vapor-phase alteration, and welding history also vary from unit to unit and within units. Intracaldera lavas and shallow volcanic intrusive rocks, moreover, exhibit even greater diversity of chemical and textural properties.

The climate within the Basin and Range province of southern Nevada is semi-arid. Rainfall averages 4-8 inches annually. Vegetative cover at the three sites is nominal to sparse. Imagery scene selection was controlled to further eliminate vegetative interference. Vegetative types include scrub evergreen trees and shrubs at some of the higher elevations and mesa tops (Kane Springs Wash only), sage brush, atroplex, box brush, foxtail grass, cheat grass, and succulents (mostly at Kane Springs Wash), including cholla and yucca.

KANE SPRINGS WASH

Kane Springs Wash volcanic center is located in southern Lincoln, County approximately 70 air miles NNE of Las Vegas in the Delamar Mountain Range (Figures 1 and 3). Access is facilitated by an excellent graded dirt road that connects the town of Caliente due south with Federal Highway 93 about 30 miles south of Alamo. Roads within the study area are sparse, poor and unimproved. Topographic relief is moderate to high. Elevations vary from 3500 to 6500 feet.

STONEWALL MOUNTAIN

The Stonewall Mountain study site is located in western Nye County 22 air miles SE of Goldfield, Nevada. The project boundary straddles the eastern margin of the Stonewall Mountain caldera and the western margin of the Mount Helen caldera. The actual mountain of "Stonewall" itself lies west of the study

site. The property is wholly within the Nellis Air Force Base bombing Range which has "active" status throughout the year. Access is by prior arrangement with the Range Commander at Nellis in Las Vegas subject to security clearance, during brief nonactive times such as weekends or range clean-up periods, and always with military escort. Topographic relief is modest, elevation varies mostly within 600 feet with two isolated extremes at 5000 and 6000 feet. The majority of the area is relatively flat.

BLACK MOUNTAIN

The NW corner of the Black Mountain study area lies only 5 miles SE of the Stonewall Mountain project boundary. The site centers on Black Mountain and the Black Mountain caldera structure. Access is, again, as with the Stonewall Mountain site, through the commander at Nellis Air Force Base in Las Vegas. The site is a "manned area" not subject to bombing exercises, so field parties are not restricted to weekends and other rare isolated "nonactive" periods. Military escort is, however, required at all times. Topography is more rugged than within the Stonewall site. Elevation ranges from about 6000 feet on the pediment NW of Black Mountain to 7235 feet at it's summit.

METHOD OF INVESTIGATION

It was mentioned earlier that a 5-phase program was scheduled for this research project. This section will describe in some detail each major phase: field work, imagery processing, and laboratory analytical approach.

LANDSAT DATA ACQUISITION

The study areas under investigation for this project are encompassed within 4 contiguous Landsat 5 Thematic Mapper scenes (Figure 4). Table 1 lists scene IDs and satellite collection dates for products acquired under this contract. Data for all bands (1-7) were requested on computer compatible tapes (CCT's). For the most part, scenes acquired in mid-summer thru fall are of better quality due to abatement of vegetative activity and clear sky.

Scenes were read onto disk and, and preliminary examination conducted in the winter, 1985-86 at the Mackay School of Mines image processing center. Ten 1024 x 1024 pixel subscenes were selected over each study site. Cloud cover in these scenes is virtually absent and Rayleigh scatter in the lower wavelength

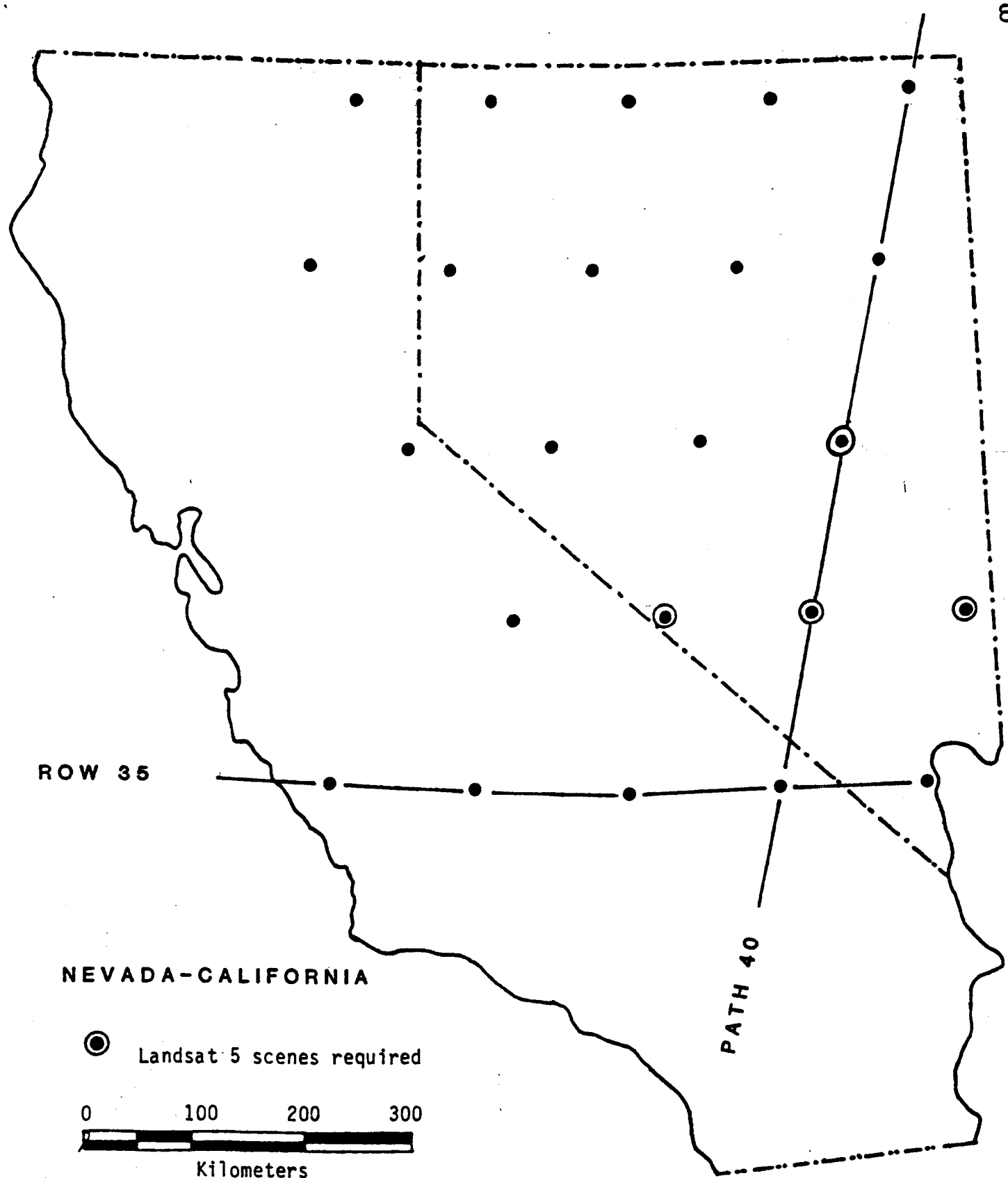


Figure 4 Landsat 5 coverage required for project area.

PATH	ROW	QUADRANT	SCENE ID	DATE OF ACQUISITION	PRODUCT
39	34	1,3,4	50139-17440	July 18, 1984	P,T(no band4),N(band 4), B/W print,1:250,000
			50475-17451	June 19, 1985	P,N,B/W print,1:1,000,000
			50491-17450	July 5, 1985	P
			50539-17444	Aug. 22, 1985	P,N
40	33	3,4	50066-17481	May 6, 1984	P,N,B/W print,1:250,000
			50466-17512	June 10, 1985	P,N
			50482-17510	June 26, 1985	N
			50530-17503	Aug. 13, 1985	P,N
40	34	1,2,3,4	50466-17515	June 10, 1985	P,N
			50482-17512	June 26, 1985	P,N
			50530-17510	Aug. 13, 1985	P,N
			50546-17505	Aug. 29, 1985	P
			50578-17502	Sept. 30, 1985	P
			50594-17501	Oct. 16, 1985	P
			50562-17503	Sept. 14, 1985	P
41	33	3,4	50121-17553	June 30, 1984	P,T(bands 3,6),N(bands 1, 2,4,5,7),B/W print,1:250000
41	34	1,2,4	50409-17575	April 14, 1985	B/W print,1:1,000,000
			50457-17573	June 1, 1985	P
			50473-17573	June 17, 1985	P
			50489-17573	July 3, 1985	P
			50569-17564	Sept. 21, 1985	P,N

Table 1. Landsat 5 TM Data Acquisitions

bands is minimal. Water vapor absorption effects in bands 4, 5, and 7 appears unimportant for our study objectives. Subscenes were further reduced to 512 x 512 pixel dimensions to maximize monitor resolution and data integrity. These final subscenes are approximately 14.5 kilometers (9 miles) square. They adequately cover the areas of interest.

FIELD INVESTIGATION

Field studies concluded to date were accomplished in the summer, 1986 (Figures 5, 6, & 7). Over 250 samples were collected from each of the three study sites and include bags of thin chips hosting desert varnish and other secondary surface coatings, petrographic samples for character reference and thin section, and large (6 x 6 inch) slabs for spectrographic analysis as well as coating samples. Each site was described in a field notebook and each site photographed.

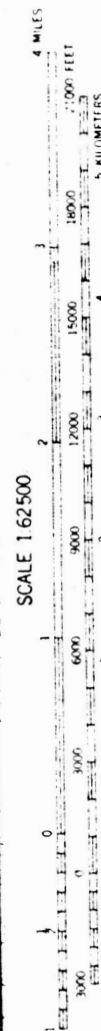
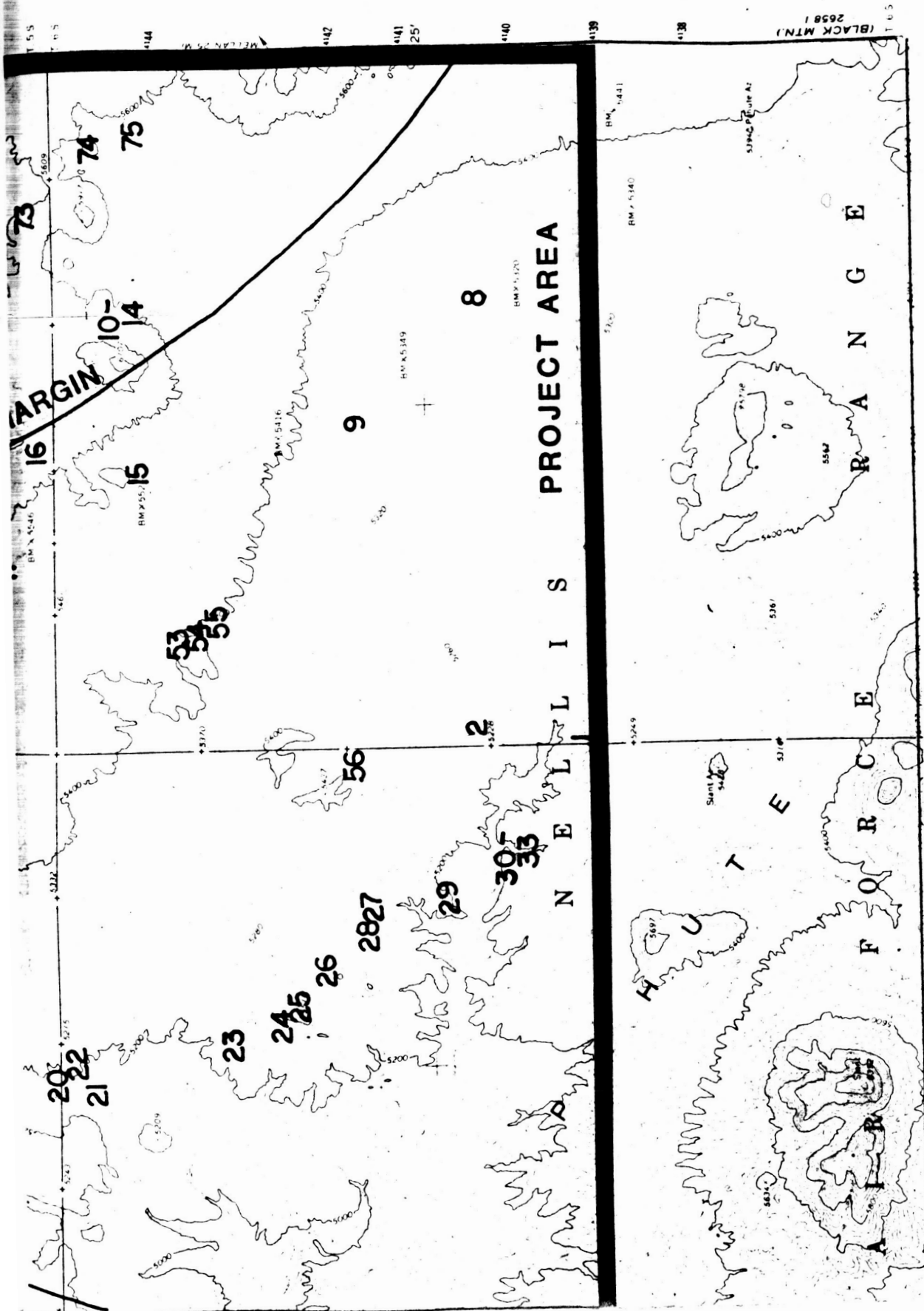
Sample sites were selected to give continuous and reasonably complete coverage from both an imagery AND lithologic unit perspective. Thus, distinct imagery units (color and gray level contrast), discerned from the initial pre-field image processing phase, were sampled as well as formationally differentiated units depicted on the geologic maps available for each area. Samples of unmapped units, including ash flow members, subvolcanic intrusives, vapor-phase altered zones, densely welded zones, and glassy tuff bases, were also sampled. A 7.5 minute topographic quadrangle base map was used for sample site notation at Kane Springs and 15 minute quads used at both Stonewall Mountain and Black Mountain. Scale of the 15 minute quads compares well with 8x10 inch enlargements of 35mm photos taken by the Dunn camera peripheral connected to our imagery processing system.

Ground-based 35mm photographs were "framed" to encompass representable scenes including outcrop, soil, regolith, and vegetation to serve primarily as reference logs to scene spectral compositions. Distance shots were also collected to show both stratigraphic relationships and sample locations.

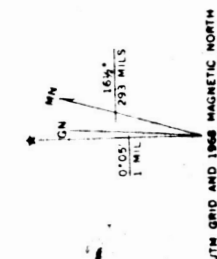
IMAGERY PROCESSING

Imagery processing was accomplished on the School's Vax 11/780 based Electromagnetic Systems Laboratories (ESL, a subsidiary of TRW Inc.) compact Interactive Digital Image Manipulation System (IDIMS) and a compact personal computer image analysis station (Table 2). The compact IDIMS offers over 250 applications functions

ORIGINAL PAGE IS
OF POOR QUALITY



CONTOUR INTERVAL 40 FEET
DOTTED LINES REPRESENT 20-FOOT CONTOURS
DATUM IS MEAN SEA LEVEL



SAMPLE LOCATION MAP-STONEWALL MOUNTAIN AREA

BASE:U.S.G.S.Topographic quadrangles, cut and spliced Fig.5

UTM GRID AND 1960 MAGNETIC NORTH
DECLINATION AT CENTER OF SHEET

ORIGINAL PAGE IS
OF POOR QUALITY

CACTUS SPRING, NEW
N3730—W11645/15

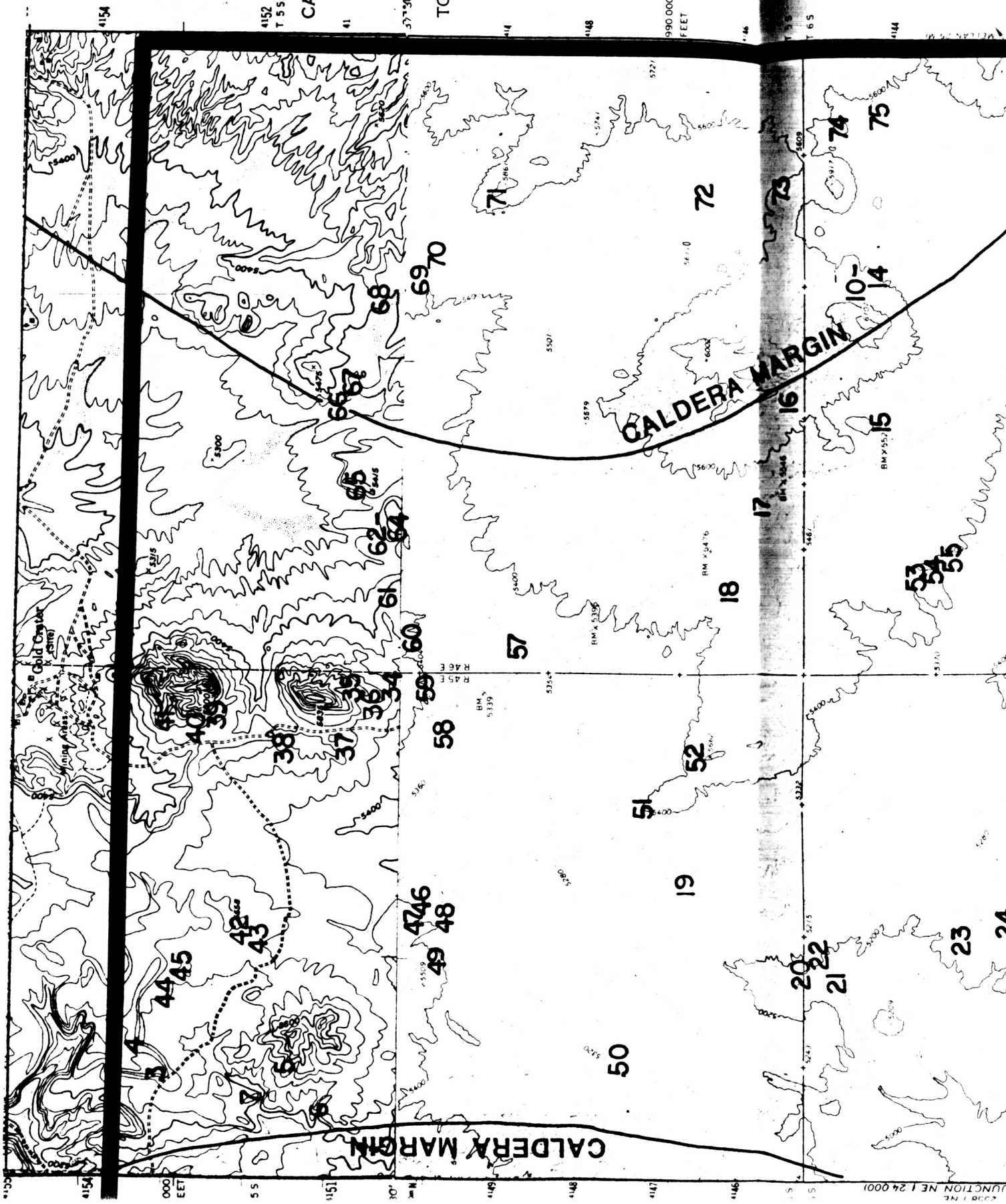
1952

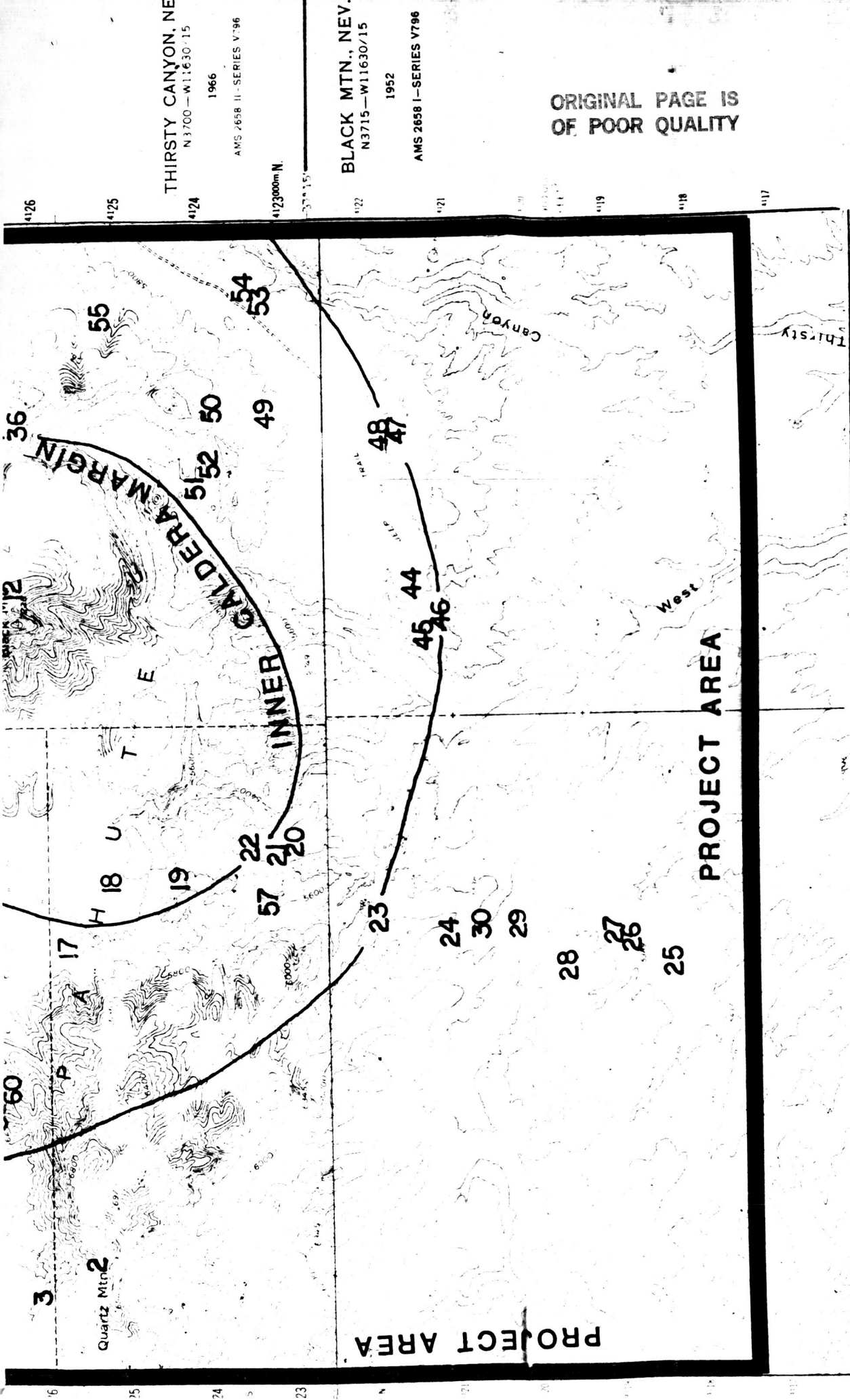
AMS 2659 III—SERIES V796

TOLICHA PEAK, NEW
N3715—W11645/15

1968

AMS 2658 IV—SERIES V796





ORIGINAL PAGE IS
OF POOR QUALITY

THIRSTY CANYON, NEV.
N 3700—W 11630/15

1966

AMS 2658 II—SERIES V-96

4123000m N

BLACK MTN., NEV.
N 3715—W 11630/15

1952

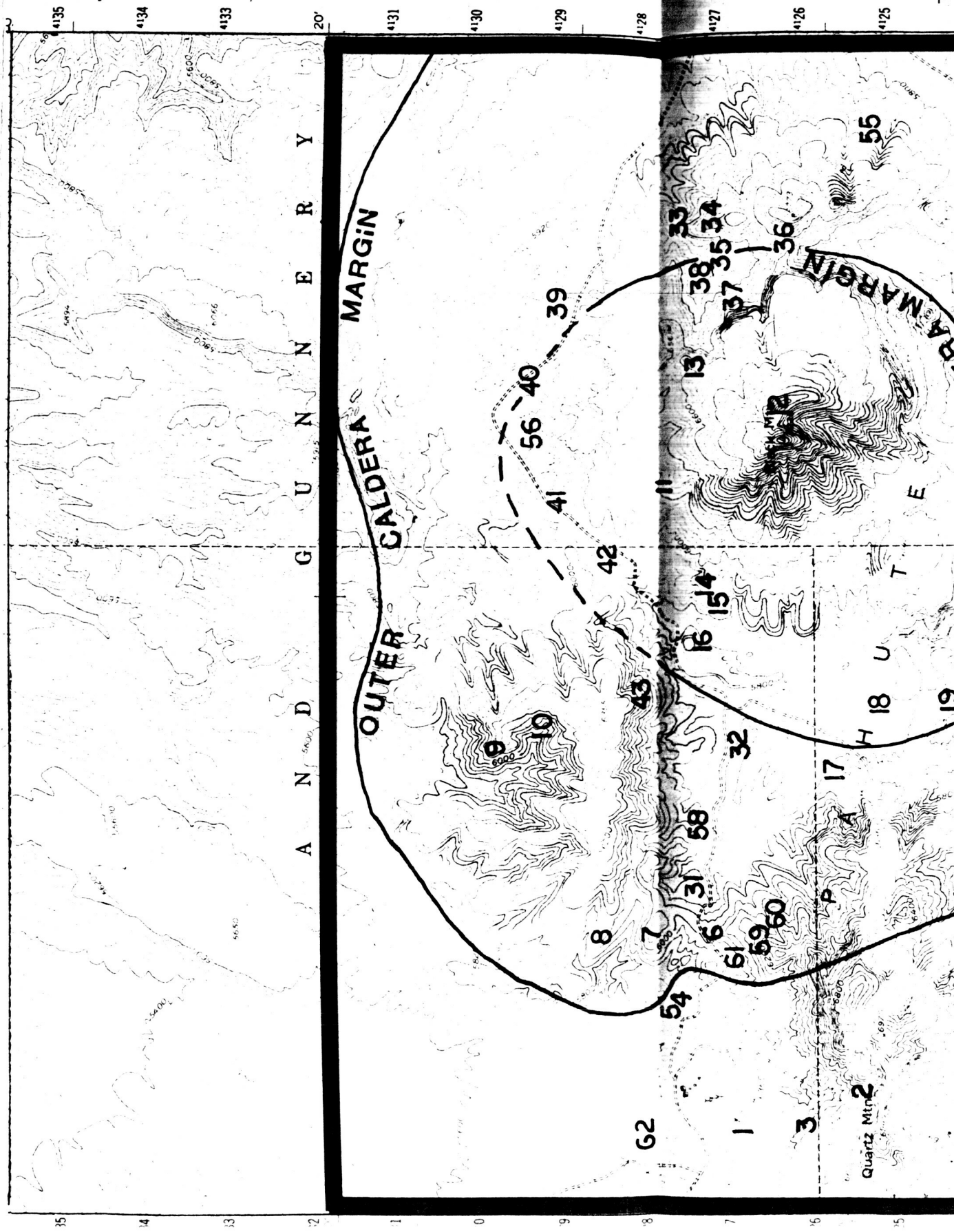
AMS 2658 I—SERIES V796

SAMPLE LOCATION MAP—BLACK MOUNTAIN AREA
BASE:U.S.G.S. Topographic quadrangles, cut and spliced **Fig. 6**

CONTOUR INTERVAL 40 FEET
DASHED LINES REPRESENT 20-FOOT CONTOURS
DATUM IS MEAN SEA LEVEL

UTM GRID AND 1942 MAGNETIC NORTH
DECLINATION AT CENTER OF SHEET

ORIGINAL PAGE IS
OF POOR QUALITY



MARGIN

ORIGINAL PAGE IS
OF POOR QUALITY

19 18

17

20

16

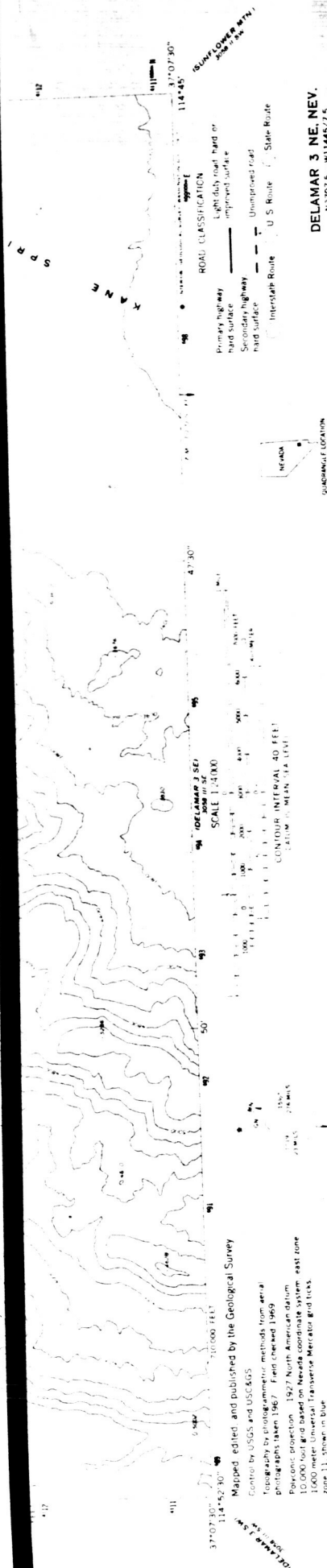
15

PROJECT AREA

51

52 60

53 59

54 56 57 58
55

SAMPLE LOCATION MAP-KANE SPRINGS WASH AREA

BASE: U.S.G.S. Topographic quadrangle, reduced 50% Fig.7

ORIGINAL PAGE IS
OF POOR QUALITY

PROJECT AREA

CALDERA MARGIN

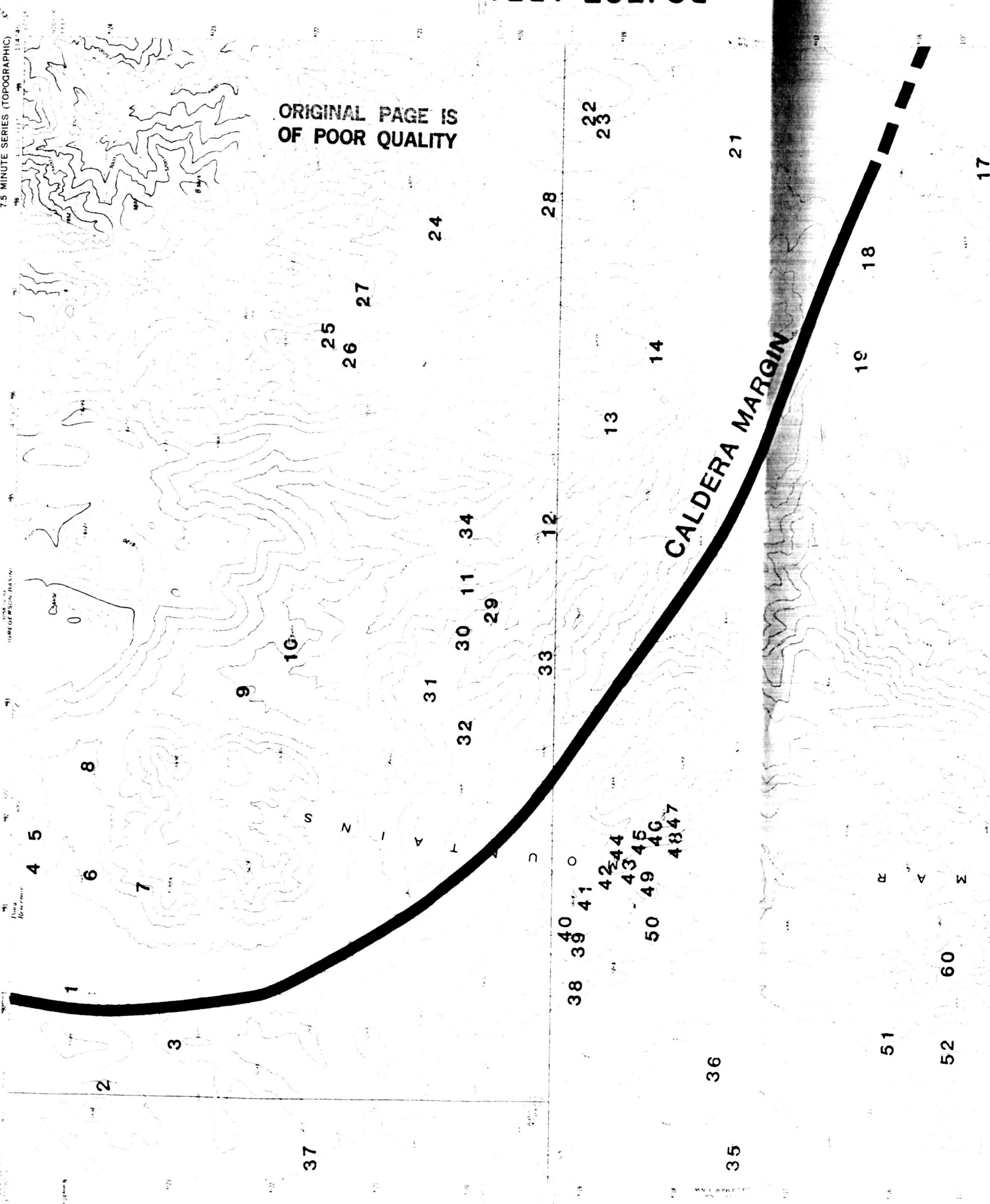


TABLE 2

FACILITIES AND DATA PROCESSING EQUIPMENT

Mackay School of Mines has acquired a VAX-based Electromagnetic Systems Laboratories (ESL) Interactive Digital Image Manipulation (IDIMS) System and a personal computer image data analysis laboratory consisting of the following:

<u>Manuf.</u>	<u>Model</u>	<u>Description</u>
DEC	780XA-AE	VAX 11/780 CPU with 8 MB memory, (256KB Boards)
DEC	BA-D0-11	Expansion Box and expansion backplane
DEC	FP780-AA	Floating Point Accelerator
DEC	RUA81-CA	456 MB Fixed Disks (2 each)
DEC	RUA60	205 MB Removable Disk
SI	9700-53	800/1600/6250 BPI, 125 ips Tape Drives (2 each)
DEC	A100-BA	Decwriter Terminal
DEC	VT100-AA	2-Video Terminals
DEC	LP11-AA	300 lpm Printer
DEC	11/24-DC	LSI 11/24 Controller with 1MB Memory
DEANZA	IP8500	Gould-DeAnza Image Array Processor
DEANZA	IP85-M	8-Image Memory (512x512x8 Bit) Planes
DEANZA	IP85-DVP	Digital Video Processor with Tracball and Assoc. Interfaces
CONRAC	7211	19" High Resolution Monitor
ESL	-----	IDIMS, GES, ERIS, Data Catalog Software License
DEC	QE100-VZ	Fortran License
DEC	QE126-VZ	Pascal License
DUNN	634	Color Camera
CALCOMP	9160	Digitizing Station
DEC	DECNET	Ethernet
SYNTAX	SP-245/253	Network Software
3 COM	501C	Network Hardware
IBM	P-AT	IBM PC-AT with 30 MB Hard Disk No. 9 Graphics Board, AST Preview Card, Monochrome Monitor, Electronome Color Monitor, Summouse, and 80287 Chip, (16 Terminals)
MDA	MERIDIAN	MacDonald Detweiler Interactive Display and Analysis Software

implemented by command language or menu.

Prior to conducting any field work and in advance of any significant knowledge of the areas under investigation, image processing was conducted on each of the 512 x 512 subscenes described in the section on "Data Acquisition" above. This a-priori approach was intended to result in unbiased remote sensing units by objective processors. Field sampling was then partially based on these pre-field images, sample sites selected to include remote sensing units distinctive in terms of color, tonal, textural, or pattern characteristics. Further imagery processing was then conducted in the fall of 1986, after the previous summer's field work. The aim of subsequent imagery manipulation and assessment has been to refine enhancement techniques and contrast between rock units with benefit of direct field experience with coatings and lithologies.

For each subscene the following images were produced and photographed with the system's Dunn camera peripheral on 35mm film:

INDIVIDUAL BANDS: 1,2,3,4,5,7
 BAND RATIOS: 4/3, 3/1 or 3/2, 5/1 or 5/2, 5/7
 SIMPLE COMPOSITES: 3-2-1, 3-5-7, 1-3-5, 3/1-5/7-4
 ISH: individual intensity(I), saturation(S), hue(H)
 on bands 3-5-7 and 1-3-5
 ISH COMPOSITES: 3-5-7, 1-3-5, 1-2-4, 2-4-5
 PRINCIPLE COMPONENTS: individual PC's 1,2,3,4,5,&6
 COMPOSITE PC's: 1-2-3, 2-3-4, 1-2-4, 1-2-5, 2-4-5
 COMPLEX COMPOSITES: 3-5or7-I,S,or H (1-2-4);
 3/1-7-I,S,or H (2-4-5);
 3/1-5/7-I,S,or H (2-4-5);
 3or3/1, 5or5/7, PC1or2;

Although image composites other than those listed above were reviewed, these band relationships and imagery renditions are thought to represent best contrast relationships between lithologies and should enhance coating characteristics inasmuch as emphasis is placed on the "alteration" bands, bands 3 and 7. Band 5 is a well established high contrast spectral interval for most cover types, especially lithologies with regard to divalent iron content. Each individual band image and composite was contrast stretched, linearly, using the IDIMS scaling function (described below) at a .5 truncation. All composites were color encoded red, green, blue (left to right). Some of the more effective images were edge enhanced by a kernel convolution technique described below.

The following list provides a brief description of the IDIMS functions utilized for this project and

should help clarify captions on images presented in following sections. Discussions of image enhancement techniques have been presented by Taranik (1978b) and Sabins (1987).

SCALE. Each band was linearly stretched using IDIMS function "scale". Whereby an arbitrary amount of both the high and low tails of the brightness range distribution of pixels for each band is assigned to the maximum and minimum values respectively, and remaining intensity values stretched throughout the complete scale of 256. For final computation a histogram is calculated by the function. Experimentation yielded a consistently attractive value for truncation of 0.5 for most image manipulation applications. For principle component analysis, however, a truncation value of 0.2 proved superior. The result is a contrast enhanced image with brightness values extending the entire range of system resolution capacity, thus providing maximum brightness contrast between cover types.

RATIOS. Band ratios (Band x/Band y) are computed through IDIMS function "divide" and involve dividing pixel intensity values in the numerator band by corresponding pixel intensity values for the band in the denominator. Resulting values tend to smooth out topographic reflectance and provide relative brightness values representative of cover type.

EDGE. Edge enhancement techniques involve either coarse or fine scale adjustments to smooth out contrast variations or sharpen them. For our purposes, the edge enhancement function sharpens remote sensing units by increasing the contrast at unit boundaries. A "kernel" is produced by IDIMS function "KERNEL" whereby a 3 x 3 pixel size area was selected and an algorithm applied to each pixel at its center throughout the scene. The algorithm involves comparing the central pixel to brightness values of the surrounding pixels to identify those with a relatively large difference. Those central pixels whose intensities do vary markedly from the average of those surrounding it are either increased or decreased in value as appropriate to increase even further the intensity difference. The kernel is moved over each pixel by the function "CONVOL". The result is to enhance the edges of imagery units relative to bordering units thereby sharpening the contrast.

ISH. The ISH transformation is a commonly applied computerized image manipulation technique which subdivides colors in color composite images into the optical parameters - intensity (i), saturation (s), and hue (h) (Buchanan, 1979; Haydn, et.al., 1982). Red, green, and blue are transformed to intensity, saturation, and hue, and resulting 3 image composites

thus represent I, S, and H, rather than the individual input bands. (There are 3 input bands.) The IDIMS function ISH applied throughout this project plots the three primary colors at the vertices of an equilateral triangle. Intensity is defined as the average of the intensities of each color (each of the original bands). Saturation indicates the purity of a color with respect to departure from achromatic (white) which plots at the center of the triangle. Saturation would thus be at a minimum at the center, a maximum on the triangle periphery. Hue is defined in relation to color. It begins at red (minimum), increasing toward green and then blue, and up to a maximum at red again. Each parameter - I, S, and H - range from 0-255. An RGB function IDIMS converts ISH to red, green, blue.

PRINCIPLE COMPONENTS. Descriptions of principle components statistical analysis (PC's) are given by Davis (1973) and Joreskog, et.al. (1976). Application to remote sensing imagery transformation has been described by Fontanel, et.al. (1975); Podwysocki, et.al. (1977); and Taranik (1978). PC's, the basis of modern factor analysis schemes, are the eigenvectors of a variance-covariance matrix. The variance of two variables, in this case intensity values of two bands, is plotted on an x-y coordinate system. A point is then located perpendicular from each coordinate at the variance value extending a distance equal to the covariance. An ellipse is plotted with its center at the coordinate origin and bound near one end by the two points. The vector from origin to the apex of the ellipse is PC1 and all intensity values are regressed to that vector. PC2 is perpendicular to PC1, extends through the coordinate origin, and is bound by the ellipse. It is always much shorter than PC1 and resultant intensity values considerably lower. Podwysocki (1977) describes resultant values as "new variables (components) which are linear combinations of the original variables; each component contains uncorrelated information". All six TM bands may be entered and a complex principle components analysis computed, resulting in 6 PC's. The IDIMS function KLTRANS takes a covariance matrix computed through function ISOCLS and computes PC's. The principle components transformation typically provides maximum contrast between cover types and PC composites aid distinction between lithologies, vegetation, and topographic effects.

LABORATORY RESEARCH

Analytical investigations of coatings began in the Fall of 1986 and to date over 50 thin sections have been studied to varying degrees of detail and 52 X-ray

diffraction (XRD) analyses have been completed. The suite of samples selected for both applications represents all major volcanic units present at each of the 3 study sites as well as the diverse coating types observed. Further analytical work is planned for the winter, 1986-87, should include X-ray fluorescence (XRF), scanning electron microscopy (SEM), and perhaps electron probe analysis.

THIN SECTION PETROGRAPHY. Over 70 thin sections have been prepared. Each is cut perpendicular to the rock surface, exhibiting surface coatings, and extending down into the host rock. In this geometry boundaries between surface coatings and underlying host can be observed and relationships noted. Each section was ground to 3 micrometers by a Nevada Bureau of Mines technician with explicit instructions to maintain section edges and edge thicknesses. Petrographic investigations are being conducted on a standard binocular petrographic microscope.

XRD. Coating material from surface chips of 52 representative rock units was extracted for XRD analysis. The technique employed involved briskly and lightly vibrating fine powder size material from the rock surface with an electric scribe with a carbide steel tip. Some of the extraction was accomplished under a Baush and Lomb zoom binocular scope. Although the instrument has both diamond and tungsten carbide tips available, these harder points tend to drill beneath the surface coatings into underlying fresher rock. Still, much of the coating compositions collected in this manner contain primary rock constituents. Powders were screened to 100 mesh to exclude coarser particles likely to involve underlying primary minerals, then ground in an agate mortar and pestle prior to mounting on a glass slide for X-ray analysis. Greater than 90% by volume of the particles extracted from the rocks were less than 100 mesh (0.147mm) in size. In view of the method applied it is felt that little material beyond this thickness (0.2mm) contaminates the samples.

All samples were X-rayed on one of Mackay's Philips Norelco XRD instruments and 2 theta measurements calibrated to a known quartz standard. Samples were saved in numbered glass vials.

LANDSAT IMAGERY APPLICATIONS IN TERRAIN ASSESSMENT

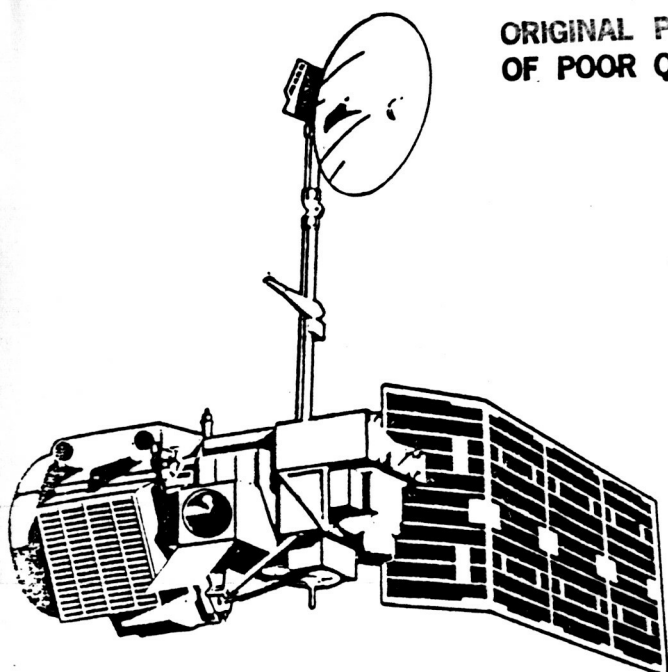
Descriptions of the Thematic Mapper remote sensing system have been presented by Engel (1980), Engel and Weinstein (1982), Engel et.al.(1983), and Sabins (1987) (Figures 8 & 9). Taranik (1978a) and Taranik and Trautwein (1977) describe in detail geologic remote sensing applications of Landsat multispectral data. Computer processing techniques were further outlined by Tananik (1978b). A series of papers by Hunt (1977); Hunt and Ashley (1979), Hunt and Salisbury (1970), and Hunt, Salisbury, and Lenhoff (1973a, 1973b, 1973c, and 1974), present compilations of spectral data and mineral and rock spectral libraries for visible and near-infrared reflectance. Earlier work on silicate mineral spectra was published by Clark (1957).

Computer processing techniques using appropriate spectral relationships enhance select lithologies and surface alteration types. Overall rock reflectivity tends to increase in the visible and near-IR interval of the electromagnetic spectrum to a maximum usually at about 1.5 micrometers (TM band 5). Reflectivity of reddish colored iron oxide minerals is greatest in the red portion of the visible spectrum - .6-.7 micrometers (TM band 3). Secondary clay minerals, which exhibit relatively intense reflectiveness throughout the visible spectrum, register a *Rehstrahlen* absorption peak at about 2.2 micrometers (TM band 7). Other hydrous minerals, sulfates, and carbonates possess similar spectral properties, with absorption minima also near 2.2 micrometers.

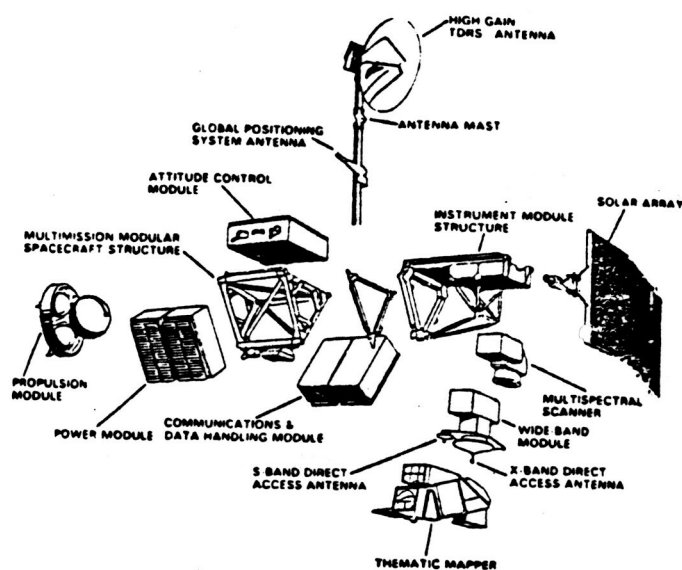
By selecting bands positioned where maximum spectral contrasts occur between surface cover, computer enhancement techniques can be exercised to highlight tonal contrast or provide distinctive color tones in the case of false color composites (Taranik, 1978b and Trautwein and Taranik, 1978). Lithologic discrimination with visible and near-IR spectra can be achieved on the basis of iron content (Baird, 1984a and 1984b, and Rowan et.al., 1974 and 1977). Discrimination of hydrothermal and supergene alteration using narrow band visible and near-IR reflectance data has been reported by Abrams et.al.(1977), Farr (1981), Podwysocki et.al.(1983), and Segal (1983). The ISH transform has been successfully applied to TM data for cover type discrimination notably recently by Borengasser et.al.(1984) and Haydn et.al.(1982).

Manipulation of bands and transform images in various combinations by both trial and error and concentration on spectral bands with unique properties helped identify certain bands, complex transformations, and hybrid image combinations that provide superior

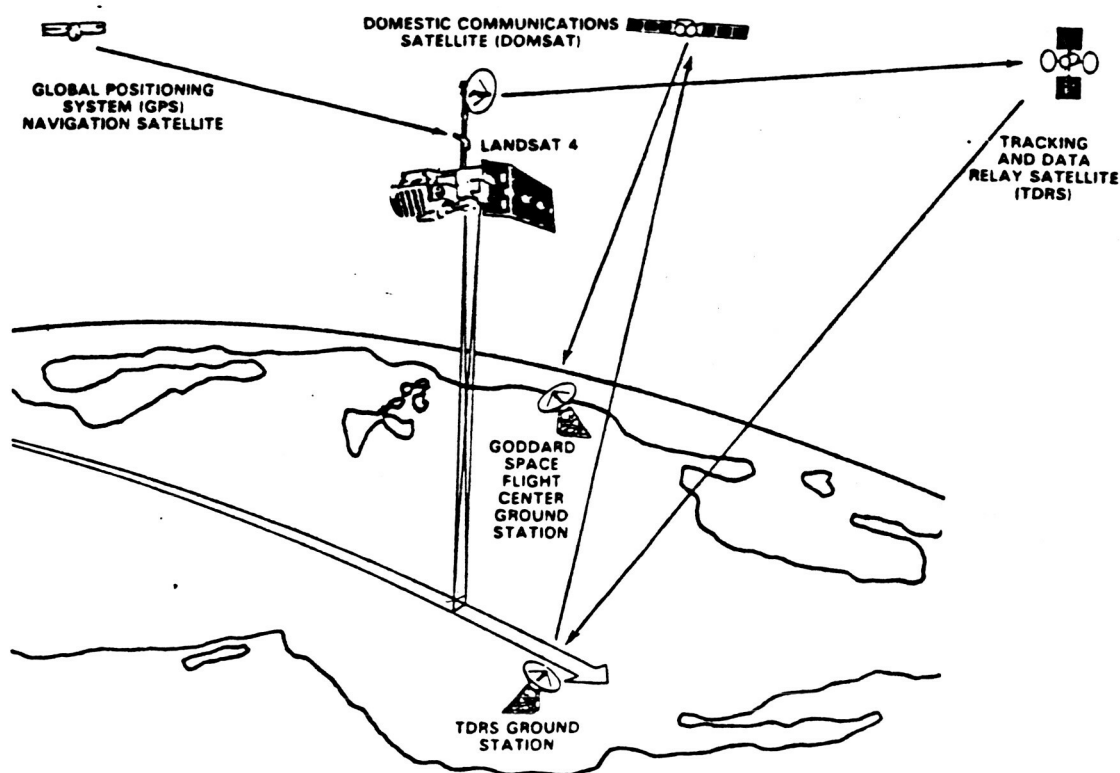
ORIGINAL PAGE IS
OF POOR QUALITY



Satellite platform of Landsats 4 and 5.

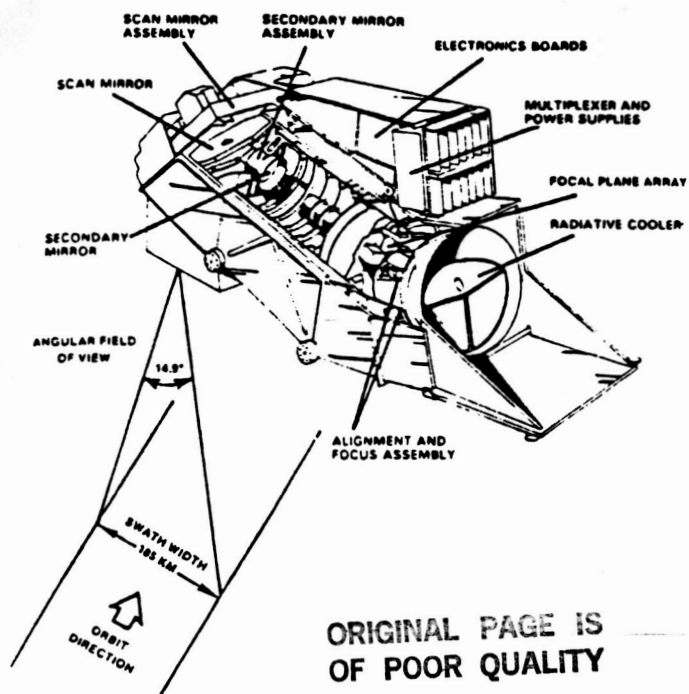


Components of the platform of Landsats 4 and 5.



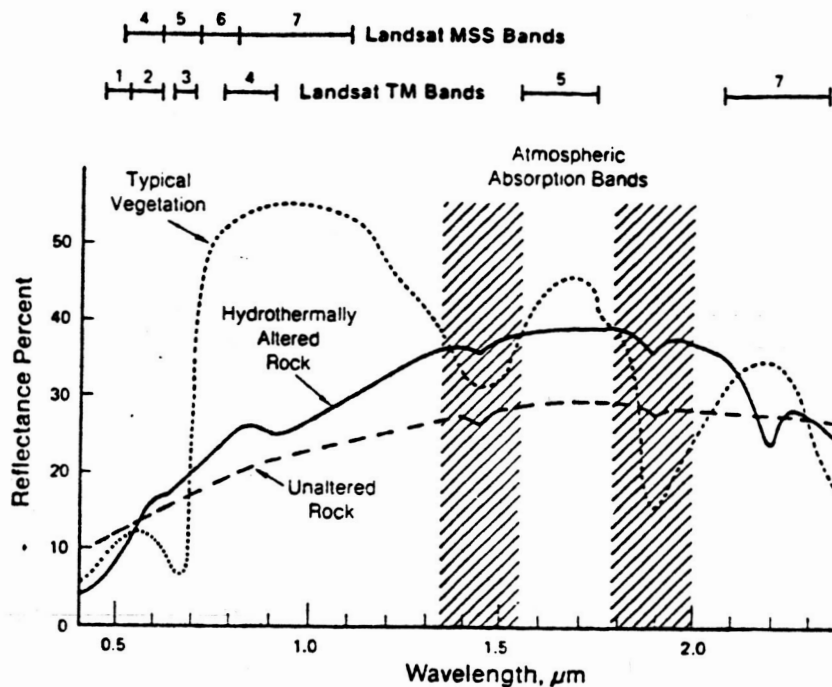
Communications network for Landsats 4 and 5.

FIGURE 8 (After Sabins, 1987)



ORIGINAL PAGE IS
OF POOR QUALITY

Thematic-mapper system.



Spectral bands for TM and MSS systems. Reflectance curves for vegetation, unaltered rocks, and hydrothermally altered rocks. From Sabins (1983, Figure C-5).

Thematic-mapper spectral bands

Band	Wavelength, μm	Characteristics
1	0.45 to 0.52	Blue-green—no MSS equivalent. Maximum penetration of water, which is useful for bathymetric mapping in shallow water. Useful for distinguishing soil from vegetation and deciduous from coniferous plants.
2	0.52 to 0.60	Green—coincident with MSS band 4. Matches green reflectance peak of vegetation, which is useful for assessing plant vigor.
3	0.63 to 0.69	Red—coincident with MSS band 5. Matches a chlorophyll absorption band that is important for discriminating vegetation types.
4	0.76 to 0.90	Reflected IR—coincident with portions of MSS bands 6 and 7. Useful for determining biomass content and for mapping shorelines.
5	1.55 to 1.75	Reflected IR. Indicates moisture content of soil and vegetation. Penetrates thin clouds. Good contrast between vegetation types.
6	10.40 to 12.50	Thermal IR. Nighttime images are useful for thermal mapping and for estimating soil moisture.
7	2.08 to 2.35	Reflected IR. Coincides with an absorption band caused by hydroxyl ions in minerals. Ratios of bands 5 and 7 are potentially useful for mapping hydrothermally altered rocks associated with mineral deposits.

FIGURE 9 (After Sabins, 1987)

enhancement qualities. It is obvious that in remote sensing we are detecting surficial spectral phenomenon. Inasmuch as band 3 provides special spectral properties of the iron oxide minerals and band 7 exhibits unique absorption characteristics of clay and other secondary hydrous minerals, it seems reasonable that these bands might provide improved contrast for our purposes. Band 5 has proven to be the most consistently effective discriminator of various cover types. We have found that these 3 bands provide the best spectral contrast between lithologies of the 3 project areas. Combining these 3 bands with enhanced composite images; ratioing them with appropriate low intensity counterparts and combining them with complex transformations seem to bring out the best (with current technology) color contrast relationships between lithologies. Principle components analyses are especially effective image transformations. PC1 contains by far the majority of variance between bands largely as a function of topographic reflectance effects. It is a very high contrast single "band" image. Variance remaining in reflectivity data beyond PC1 are essentially devoid of topographic effects and seem to exhibit more reflective intensities dependent directly on surface cover. PC3 corresponds quite closely with 4/3 ratios, which tend to enhance vegetation spectral effects. Vegetation tends to be very bright on 4/3 images.

It appears that the variance remaining in PC3, 1 in PC2 correlates closely with lithologic variation without topographic interference. ISH transformations seem to work best in the project area with bands 3, 5, and 7, the surface cover and alteration bands, if you wish. By combining ISH transformations with individual bands or band ratios (always stretched) high contrast images can be displayed. It is important to use nonrepetitive data - excluding a band from dual contribution. For example, an intensity parameter band of bands 1-2-4 would combine well with bands 3 and 5 or 7. Therefore redundancy of any band contribution to the image is illiminated. ISH saturation or hue on bands 2-4-7 in combination with bands 3 and 5 or 3/1 and 5 is another example.

MINERAL COATINGS IN DESERT ENVIRONMENTS

Early attempts to describe mineral coatings in desert environments (desert varnish) in a comprehensive fashion were published by White (1924), Laudermilk (1931), and Engel and Sharp (1958). A more quantitative approach to the study of coatings began in the mid-1970's and numerous workers have published their results since. Dorn and Oberlander (1981) in a fairly lengthy treatise on the topic do an excellent job of summarizing work on coatings up to that time.

Desert varnish is usually defined as the arid secondary phase of the weathered surface of rocks in arid to semi-arid environments. Taylor-George, et.al. (1983) define desert varnish as a coating of ferromanganese oxide and clay. Perry and Adams (1978) found that varnishes they studied consisted of alternating bands with variable detrital minerals of clay, feldspar, quartz, and hematite. According to Dorn and Oberlander (1981), desert varnish averages 10-30 microns thick. To most field geologists desert varnish is that conspicuous dark rusty brown to shiny black stain that commonly coats prominent desert bluffs. Iron and manganese oxides are the distinctive components.

The term coating is used here, rather than desert varnish. Mineral coating is herein defined as any inorganic secondary mantle or weathering product that occurs on the outer surface of rocks to an indefinite depth and conceals to some degree fresh, primary lithologies. Coatings may consist of secondary replacement products developed by hydration, hydrolysis, or metasomatic ionic exchanges with primary rock minerals, or precipitated or attached exogenous material. The composition of any inorganics present is not to be treated except inasmuch as they help control the origin of mineral coatings.

For purposes of remote sensing, we are concerned with the entire surface of any rock exposure, which may include both true desert varnish, subvarnish alteration zones, and relatively fresh rock with or without an incipient phase of alteration. Any given scene typically contains a combination of rock surface types, depending on host composition, textures, and topographic occurrence. Previous workers who have attempted to establish absolutes with regard to ultimate source of varnish constituents diverge on conclusion. Engle and Sharp (1958) concluded that the components of desert varnish are derived from the underlying host rock, whereas Dorn and Oberlander (1981) state flatly that the constituents of "all rock varnishes" are derived from sources external to the host rock. Source of varnish constituents and relative

proportions of exposure of varnish to underlying rock bear significantly on remote sensing interpretations.

Varnish and probably all coatings seem to require considerable time to form. Hunt (1961) sights archeological evidence to establish a threshold of about 2000 years for noticeable development. Exceptions may occur, however, and Engle and Sharp (1958) note one locality with noticeable varnish development over a 25 year period. Coatings tend to be amorphous and have a dark brown streak. Hardness of typical coatings on rocks of the Mojave Desert were measured at 4.5-5 (Laudermilk, 1931). Coatings adhere to their host tenaciously. They are insoluble in water, but readily soluble in hot, dilute hydrochloric acid. Varnishes are described to overly light "limonitic" staining and light clay alteration.

Coating morphology varies from paint-thin films to lamellar successions of light and dark layers. Borns, et.al. (1980) observed microorganisms, either mold or fungus, with a scanning electron microscope (SEM) in lamellar type coatings. Staley, et.al. (1982) describe abundant microcolonial structures of lichen, algae, and fungi on desert rock surfaces from the southwest U.S. They point out that lichen and algae can derive their nutrients from their host, but fungi require an external source and speculate that that external source is probably wind blown dust. By analysis with SEM-EDAX (energy dispersive X-ray system), Taylor-George, et.al. (1983) discovered Fe, Al, and Si, three of the characteristic elements of varnish, in fungi on rock surfaces from the Sonoran Desert. They also identified manganese oxidizing bacteria in the varnish as well. Perry and Adams (1978) found cyclic manganese deposition in lamellar coatings.

Comprehensive chemical data on varnishes were published by Engel and Sharp (1958). Their wet chemical determinations from rocks of southern California established O, H, Si, Al, Fe, and Mn as the chief elemental components. Spectrographic analyses discovered that Ti, Ba, and Sr were present in unusually high concentrations followed by other trace metals whose relative amounts seemed dependent on local geology. Compositional analysis of coatings by SEM reveals an MnO₂ concentration of up to 25% by weight (Hooke, et.al., 1969; Allen, 1978; and Perry and Adams, 1978). This anomalously high amount is difficult to reconcile given background MnO₂ concentrations in rock, soil, and dust on the order of 0.1%. Biological concentration is usually evoked to account for the MnO₂. SEM analyses by Hooke, et.al. (1969) on varnishes from Death Valley revealed an outer layer rich in Fe and Mn, with Mn/Fe increasing toward the surface, and

an inner zone enriched in SiO_2 and Al_2O_3 . The total thickness of the varnish was 20-50 micrometers. Optical and Sem analysis by Allen (1978) on varnishes from Sonoran Desert rocks indicated high concentrations of Mg as well as Mn and Fe. This metal rich layer is approximately 20 micrometers thick and consists of a "clay-like" matrix separated from the host rock by a 1mm thick weathered cortex. The cortex is composed of unoriented microcrystals probably derived from the host. These bands, also described by Engel and Sharp (1958) are attributed to the weathering process. Allen concluded the source for the metals is external to the host.

The significant contribution of both SiO_2 and Al_2O_3 to the chemical composition of coatings is attributed by Allen (1978) and Potter and Rossman (1977, 1979) to clay minerals. Potter and Rossman feel the Fe and Mn oxides of varnish are in intimate association with mixed layer illite-montmorillonite clay minerals. They still surmise, however, that the clay minerals are probably externally derived by wind. Farr and Adams (1984) and Curtiss, et.al. (1985) discovered short lived hydrous alumina-silica coating up to 5 micrometers thick on very fresh basalts in semiarid parts of Hawaii.

Recent investigations stress a likely biological origin for desert varnishes (Krumbein and Jens, 1981; Dorn and Oberlander, 1981; Taylor-George, et.al., 1983; Staley, et.al., 1983). It was noted above that some workers propose that all elemental constituents in varnish are derived externally. Neutron activation analyses by Knauss and Ku (1980) for trace elements and radioisotopes indicated that both U and associated Th in desert varnishes from the Colorado Plateau in Utah were derived from sources external to the host rocks. In a contrary view, Glasby, et.al. (1981) hold that varnish on dolerite from Antarctica is derived by leaching of elements from the substrate. They arrive at this conclusion by comparing analyses of whole rock with varnish compositions, the later of which is not enriched in manganese as is the case with varnishes from the southwest U.S.

GEOLOGIC SETTING

All three study sites are located in southern Nevada, centrally disposed within the Basin and Range province, which is noted physiographically for alternating linear N-S mountain ranges and intervening broad valleys, produced by tensional block faulting during Tertiary time. More than 20 major ash flow sheets and 8 collapse structures have been recognized (Eckel, 1968; Ekren, et.al., 1971; and Byers, et.al., 1976). A relatively young (mid to late Miocene), chiefly silicic volcanic caldera structure with associated intracaldera lavas and tuffs and outflow sheets of ash flow characterizes each of the three study sites (Figure 10). Moreover, these 3 volcanic centers are members of a suite of unusual peralkaline rhyolitic deposits present in the western U.S. (Noble and Parker, 1974). Each area is well preserved and well exposed. Pre-Tertiary rocks consist primarily of mio-eugeosynclinal Paleozoic rocks.

STONEWALL MOUNTAIN AREA

The study area at Stonewall Mountain actually involves two caldera structures - Stonewall and the Mount Helen caldera to the east. Caldera margin faults are approximately 6 miles apart and the Landsat work scene selected for this site overlaps both. Figure 11 presents geology of the area, abstracted from Nev. Bur. of Mines Southern Nye County map.

The Stonewall Mountain caldera was first described most notably by Ekren, et.al (1971). Stonewall Mountain itself centers on intracaldera complex consisting of a complicated sequence of pyroclastics, volcanic breccias, and flow dome complex (Foley, 1978). The event was quite young, relative to the southern Nevada volcanic field in general - 6 to 6.3 m.y. (Noble, et.al, 1984; Weiss, 1985). The study site involves a two component outflow ash sheet portion of the Stonewall volcanic system. Extracaldera outflow deposits from the Stonewall Mountain caldera - The Stonewall Mountain Tuff - consists of a lower pumice rich ash flow deposit - The Spearhead Member - overlain by a thinner, typically more densely welded ash flow sheet - The Civet Cat. The Civet Cat Member was auto-oxidized and is a distinctive deep reddish maroon brown color which forms a deep chocolate brown supergene coating. These units are described in more detail in the following section. Outcrop within the Stonewall study area is subordinated by alluvium and shallow regolith. Enhanced imagery tends to emphasize talus, detritus, and regolith adjacent to outcrop.

Deposits from the Mount Helen caldera are dominated

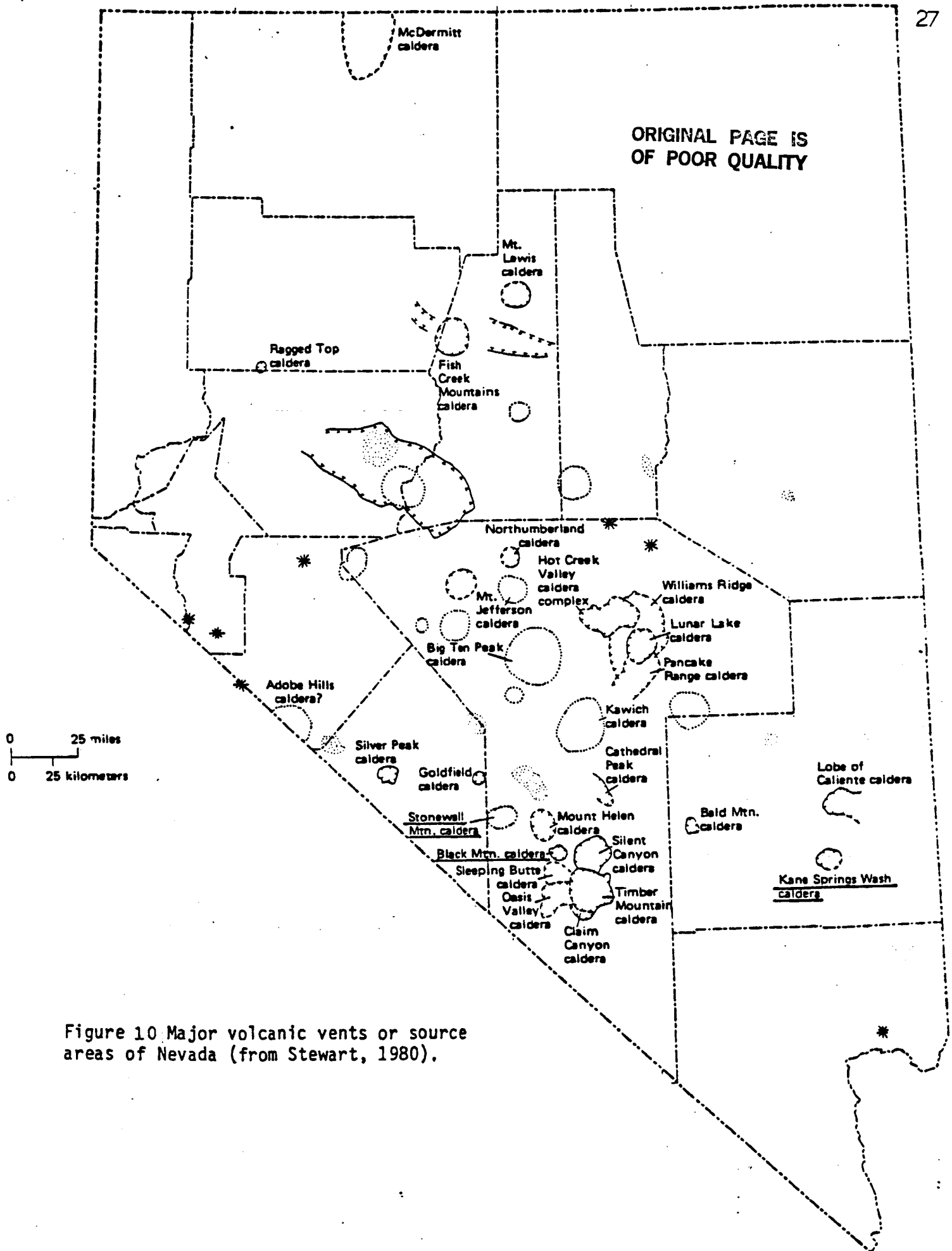


Figure 10 Major volcanic vents or source areas of Nevada (from Stewart, 1980).

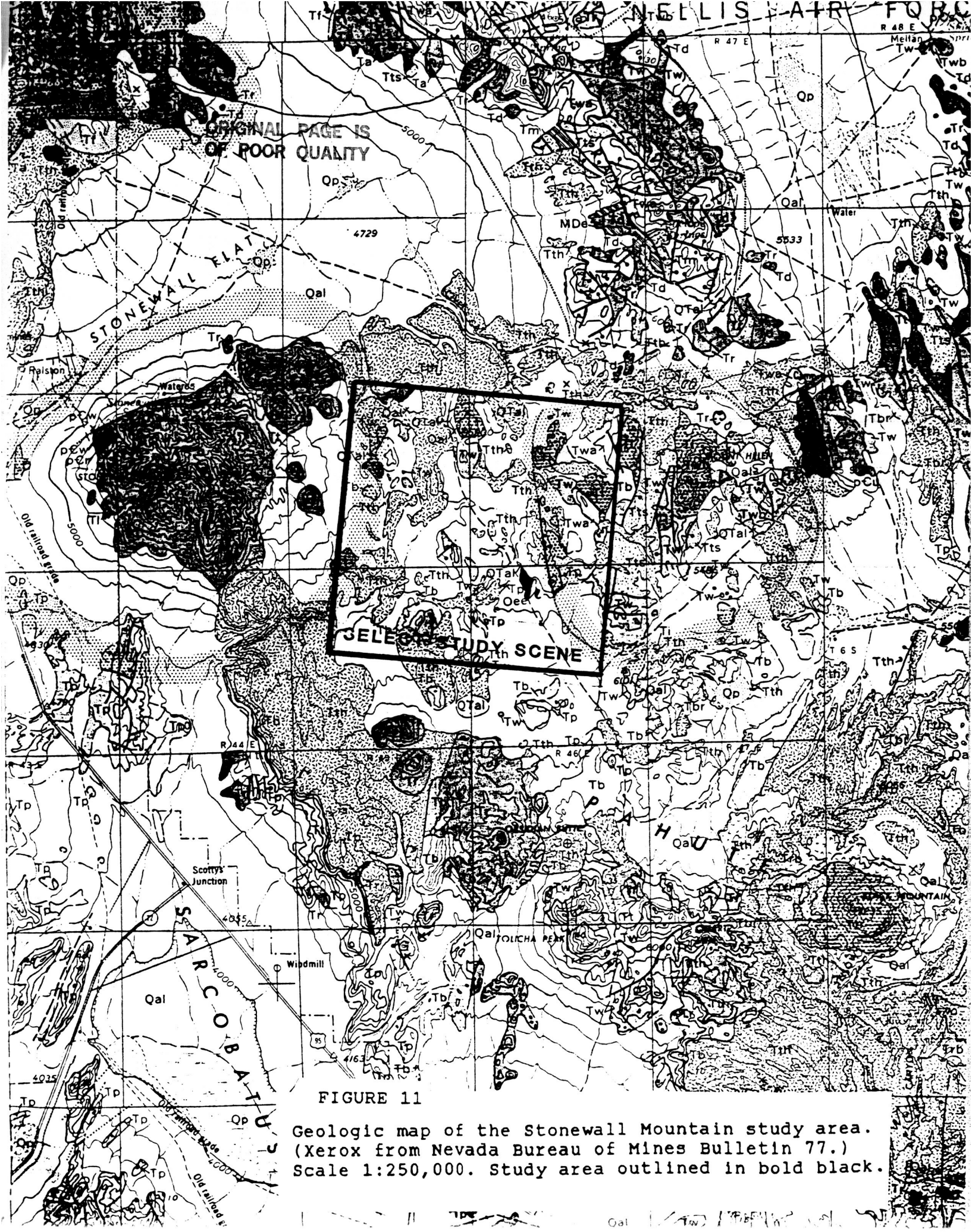
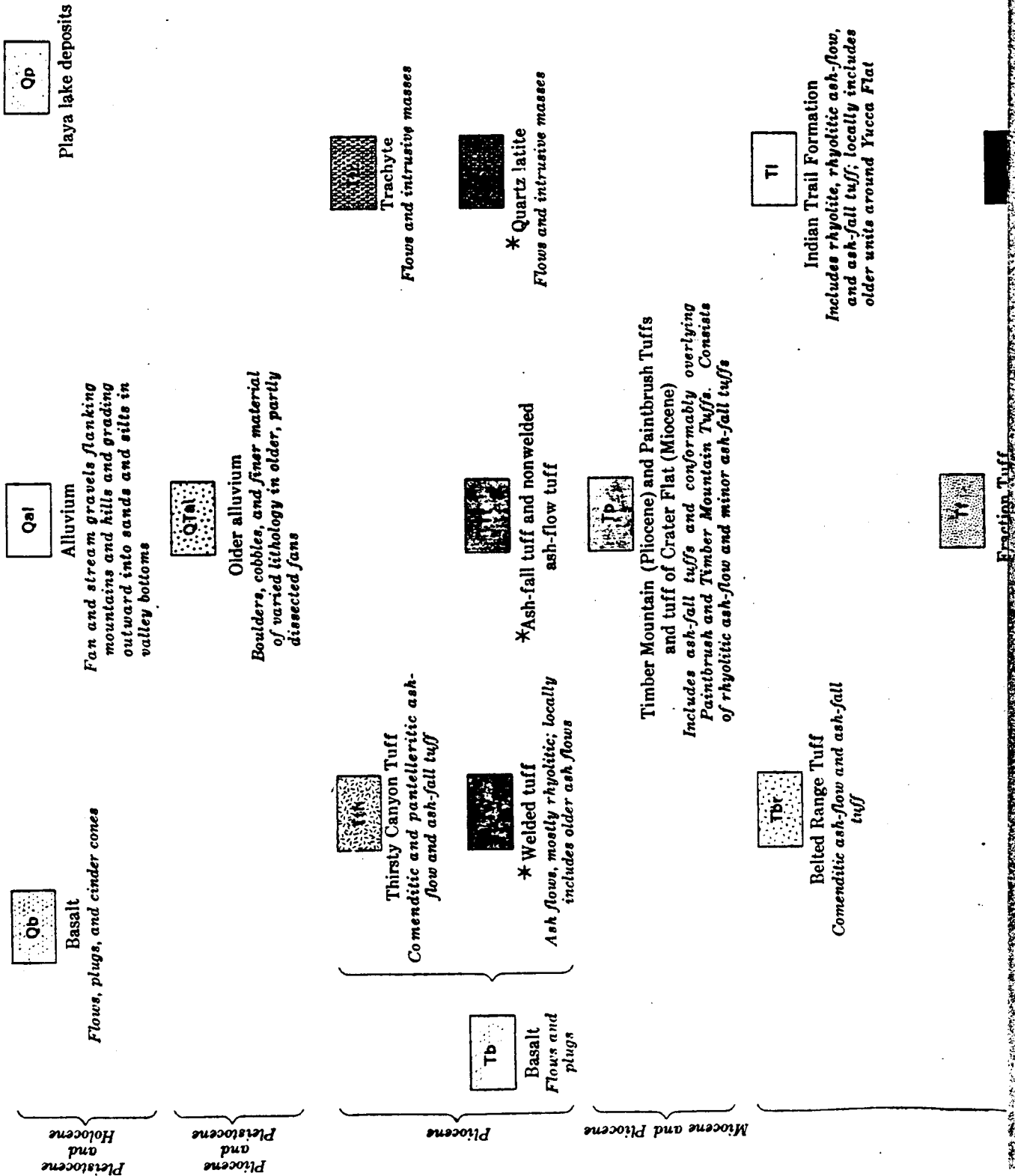


FIGURE 11 (continued). Explanation for geologic map of the Stonewall Mountain study area.

EXPLANATION



by a felsic suite of tuff and lava ranging in composition from rhyolitic to intermediate. The units are cream to pale yellow in weathered outcrop and the lavas are characterized by quartz porphyry textures. In places these felsic volcanics overly more mafic tuff and fine airfall tuff. They appear to interfinger with the Stonewall Mountain Tuff. Apparently younger basalt flows are present at two isolated locals within the work area.

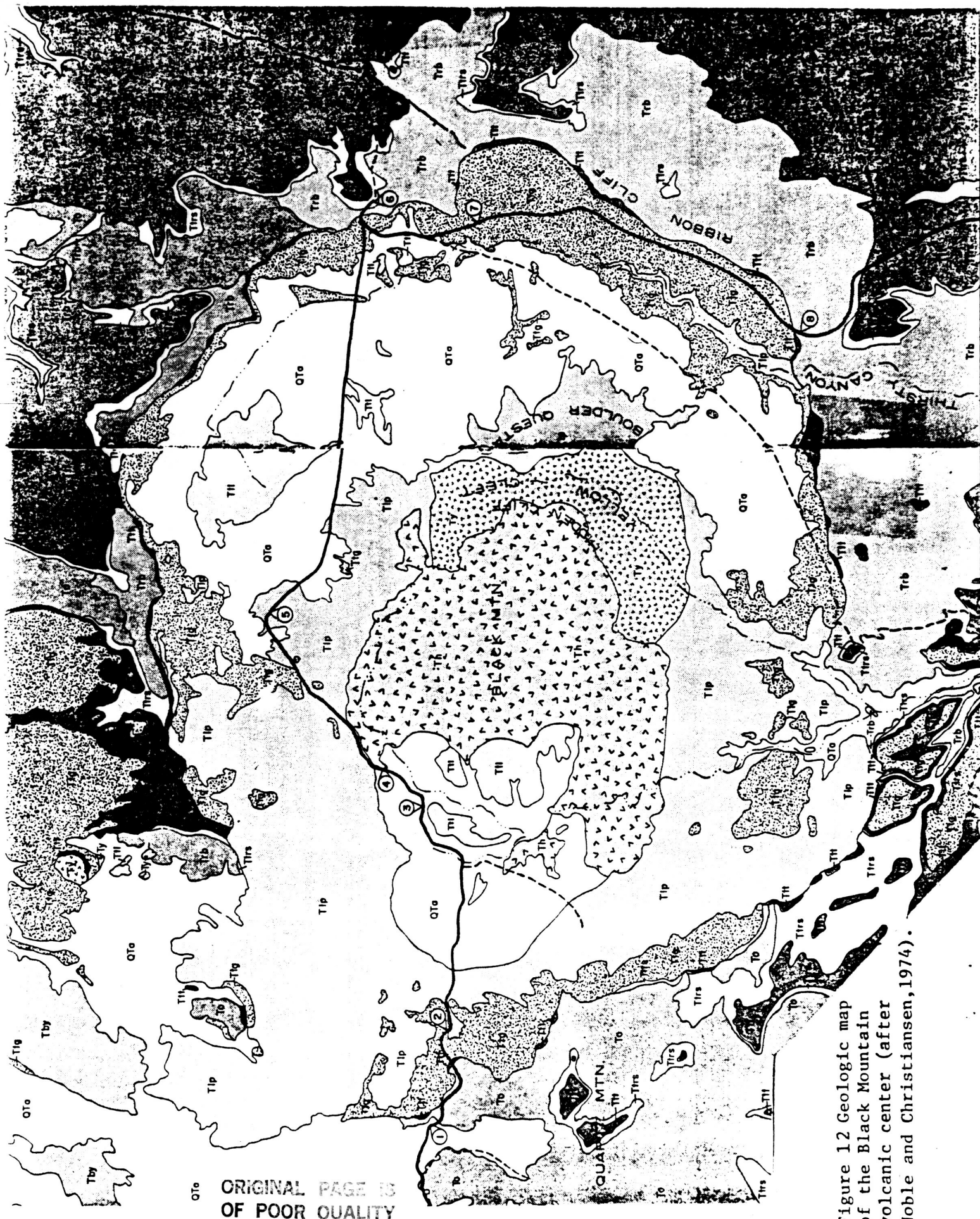
The collapsed western margin of the Mount Helen caldera is delineated by a normal fault conspicuous on both geologic maps and Landsat images. The fault is bound on the west by quartzite pebble/cobble gravels, probably old pre-caldera alluvial deposits and on the east by felsic Mount Helen flows.

BLACK MOUNTAIN CALDERA

The Black Mountain study site consists of a concise well exposed, relatively small caldera complex the margin of which is completely encompassed within the work area (Figure 12). The geology has been described by Cornwall (1972), Noble, et.al. (1964, 1968, and 1984), and Noble and Christiansen (1968 and 1974). Volcanic units are more numerous and diverse than at the Stonewall study area and were apparently produced in part by a multi-collapse sequence. The center is believed to have been active between about 6.5 to 8.5 m.y. ago.

The Black Mountain eruptive sequence overlies older lavas and tuffs, felsic in composition. One small outcrop of Paleozoic limestone occurs within the project area. The Black Mountain volcanics consist of intracaldera lavas and tuffs and an outflow sequence - The Thirsty Canyon Tuff (Noble, et.al, 1964). Table 3 tabulates volcanic and structural events at Black Mountain, taken from Noble and Christiansen (1974). Basically 3 or 4 collapse events have been recognized, each preceded by subalkaline to peralkaline lava extrusion. Collapse was attended by major ash flow eruptions, alternating initially between subalkaline to comenditic compositions with a general trend toward greater peralkalinity upsection.

The Gold Flat member is the youngest ash flow deposit. It postdates final caldera collapse and is a pantellerite by composition (Noble, 1965). The unit is a highly evolved peralkaline end member with greater than 4% iron content. The final event at Black Mountain was central volcano fill by dark trachyte and mafic trachyte lavas with peralkaline affinities. The Labyrinth Canyon ash flow deposit which occurs in an



ORIGINAL PAGE IS
OF POOR QUALITY

Figure 12 Geologic map
of the Black Mountain
volcanic center (after
Noble and Christiansen, 1974).

EXPLANATION

ORIGINAL PAGE IS
OF POOR QUALITY

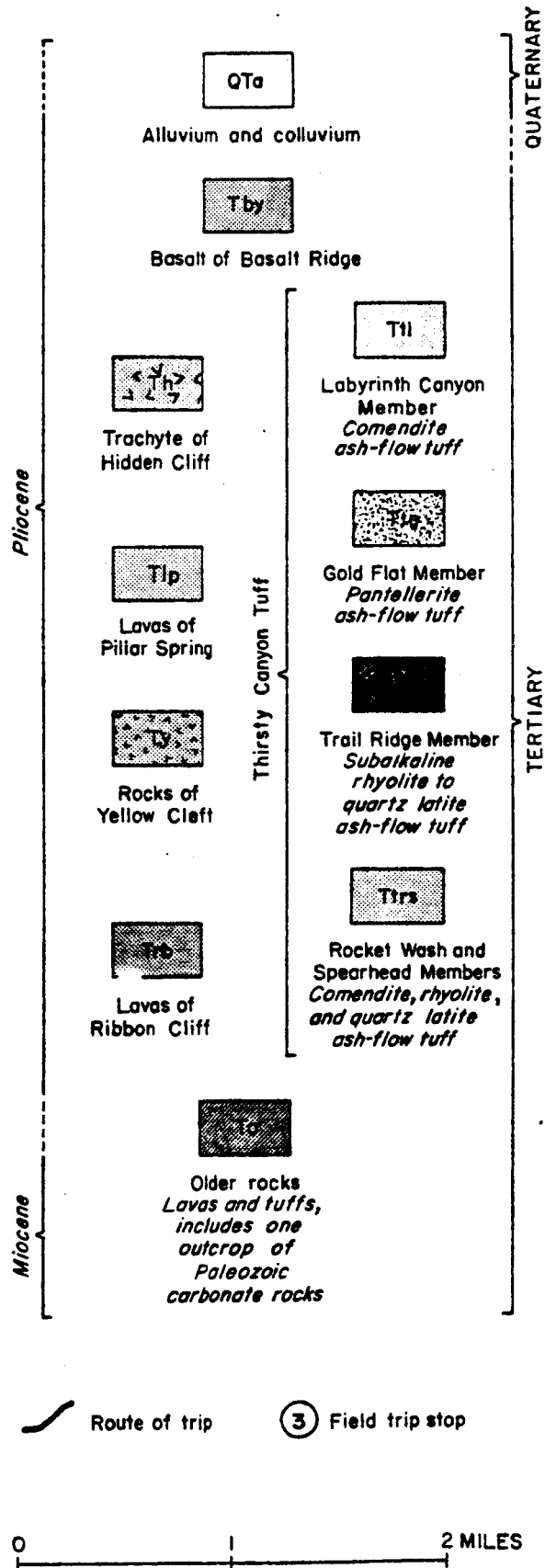


Figure 12 (continued) Geologic map of the Black Mountain volcanic center (after Noble and Christiansen, 1974), explanation.

TABLE 3

Outline of the volcanic and structural evolution of the
Black Mountain volcanic center, southern Nevada.
Arranged in ascending order of age.

Basalt of Basalt Ridge¹

K-rich hypersthene normative

Labyrinth Canyon Member of the Thirsty Canyon Tuff

Comendite; probably erupted from central vent of Hidden Cliff volcano.

Trachyte of Hidden Cliff

Trachyte and mafic trachyte with peralkaline potential; forms central volcano within post-Gold Flat caldera.

CALDERA COLLAPSE

Gold Flat Member of the Thirsty Canyon Tuff

Pantellerite produced by extreme fractionation of comendite magma.

Lavas of Pillar Spring

Trachyte with peralkaline potential; subalkaline and peralkaline silicic lavas; forms central volcano within caldera.

PROBABLE CALDERA COLLAPSE

Trail Ridge Member of the Thirsty Canyon Tuff

Compositionally zoned from subalkaline rhyolite to quartz latite.

POSSIBLE CENTRAL RESURGENCE

Rocks of Yellow Cleft and Unnamed Lavas

Trachyte and syenite with peralkaline potential to comendite; mafic trachyte; forms central volcanic complex within caldera.

MAJOR CALDERA COLLAPSE

Spearhead Member of the Thirsty Canyon Tuff

Vertically zoned upwards from comendite to quartz latite.

Unnamed Comendite Lavas

Found as lithic fragments in the Spearhead Member.

PROBABLE CALDERA COLLAPSE

Rocket Wash Member of the Thirsty Canyon Tuff

Subalkaline and/or transitional rhyolite and low-silica rhyolite.

Lavas of Ribbon Cliff

Subalkaline trachyte to quartz latite; forms a low volcanic edifice centered where caldera later formed.

ORIGINAL DOCUMENT
OF POOR QUALITY

isolated intracaldera patch on the flank of the central volcano was later recongnized by geochemical deduction (Noble, et.al., 1984) as distal Spearhead Member of the Stonewall Mountain Tuff. Detailed descriptions of all major units is presented in the following section.

KANE SPRINGS WASH

The Kane Springs Wash volcanic center was described by Cook (1966), Noble (1968). Detailed mapping and geochemical studies were conducted by Novak (1984 and 1985). Figure 13, from Novak (1984) shows area geology.

The center consists of a well defined central caldera collapse structure with a complex sequence of diverse intracaldera lavas, tuffs, and flow dome deposits that straddle the collapse event in time. The outflow formation consists of at least 8 distinct ash flow sheets, ranging in composition from subalkaline to peralkaline rhyolite with a pantelleritic trend.

The caldera rim fault is quite pronounced on the west and south edge of the caldera and marks a striking contrast between intracaldera lithologies and outflow deposits. Intracaldera deposits consist of dark trachyandesite flows primarily overlain by white pumice rich air fall tuff. Dark late basalt caps the intracaldera mesas. Intrusive through this sequence are flow dome complexes of topaz bearing rhyolite. In the NE portion of the caldera is a sequence of complexly emplaced silica poor tuffs and syenite domes which were late in the depositional history, but which do not appear to have caused resurgent doming. The outflow sheets are ash flows with typical welding, vapor phase, and vitric zonal relationships. Some air fall tuff has been recognized interstratified between ash flow formation.

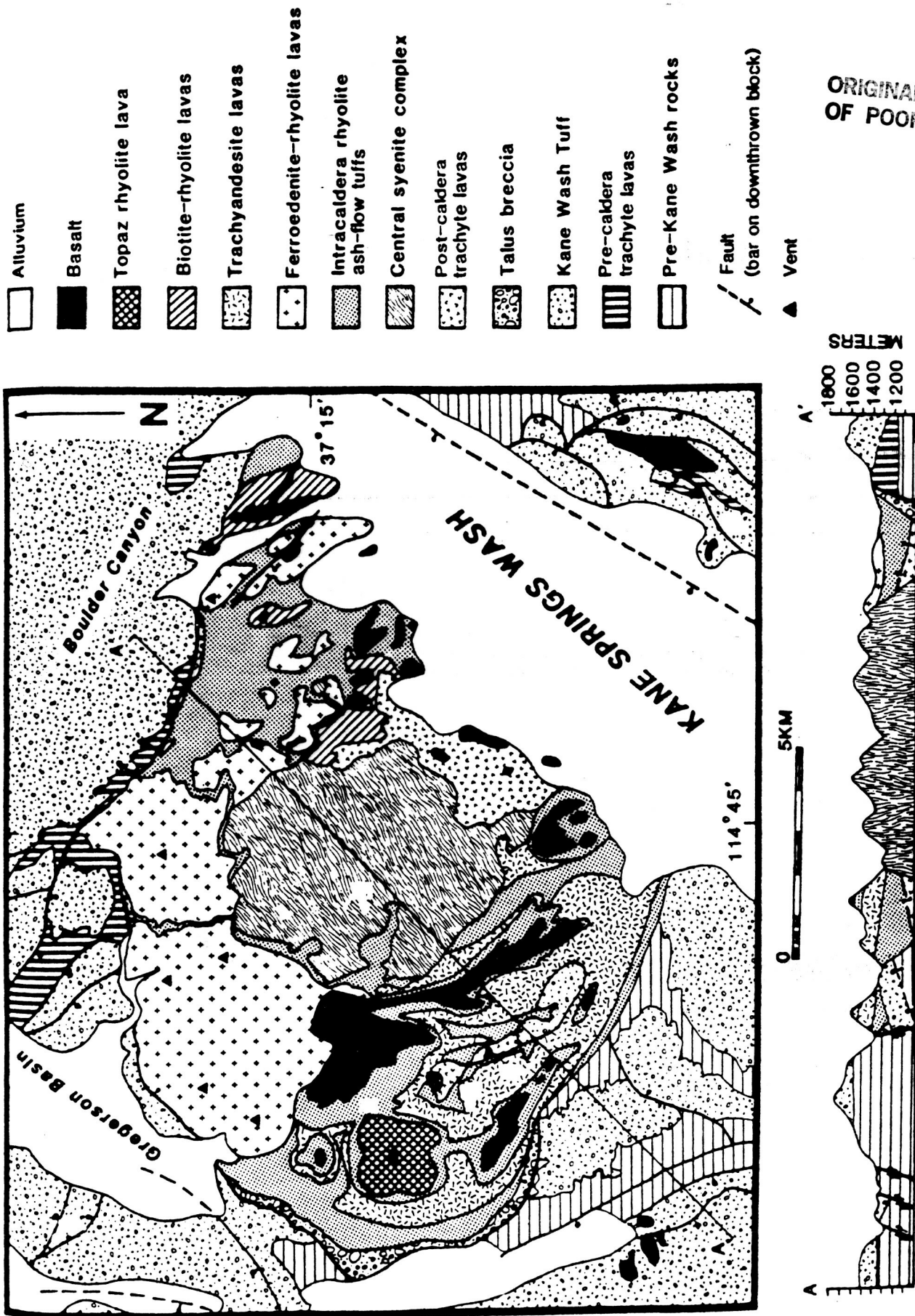
ORIGINAL PAGE IS
OF POOR QUALITY

Figure 13 Geologic map and cross section of the Kane Springs Wash volcanic center (after Novak, 1984).

INDIVIDUAL VOLCANIC UNITS

The purpose of this study was to analyze coatings on the various volcanic rock assemblages at the 3 study sites, attempt to establish the origin of the coatings, and relate the coatings to underlying host rocks and Landsat TM imagery. Inasmuch as the problem focuses largely on individual volcanic deposits rather than individual calderas or geologic settings, this section is devoted to their description. Organization is by study area and the units are described in order of decreasing age, oldest first, insofar as relative ages are known.

STONEWALL MOUNTAIN AREA

Rock units within the Stonewall Mountain Area include outflow sheets of the Stonewall Mountain Tuff and tuffs and lavas of the Mount Helen caldera. Geologic setting and references were given in the previous section. The area is covered with sparse (25 - 30% average), low plant growth, chiefly atroplex with some cheat grass. The area is unique among the 3 in monotony of vegetative cover. Significant variation appears to be virtually absent. A lively orange lichen does, however, homestead the felsic deposits of the Mount Helen center.

SPEARHEAD TUFF. The Spearhead Tuff is the lowermost member of the Stonewall Flat Tuff. In the project area the member is composed of moderate to densely welded flows of rhyolitic ash flow tuff. Outcrops are typically grayish brown to grayish tan, occurring either as dense weld prominent mesa top ledges or less welded, less resistant slope formers. The unit consists of moderate to abundant pumice fragments up to several inches in length and contains 5 to 10% phenocrysts of sanidine with minor quartz and albitic plagioclase. Rare clinopyroxene, olivene (fayalitic), sodic amphibole, and Fe-Ti oxides are also present. Geochemical investigations by Noble and Parker (1974) and Noble (1979) indicate the tuff is slightly peralkaline, very highly evolved with low Eu/Eu* and extremely low Sr, Mg, Ba, Co, and Ni. Coatings are grayish tan on moderate to poorly welded zones; very dark chocolate brown on dense weld zones.

CIVET CAT CANYON TUFF. The Civet Cat Canyon Tuff is the uppermost member of the Stonewall Flat Tuff and overlies the Spearhead Member. The two outflow sheets are separated by a lower vitric basal zone of the Civet Cat. In outcrop and hand specimen the unit is a distinctive brick-red brown to reddish chocolate color due to microscopic secondary hematite that formed

during auto-oxidation of the unit upon deposition. The unit is densely welded and granophyrically crystallized where it occurs, primarily as mesa caps, in the study area. Thicknesses range from about 2 to 5 meters. The Civet Cat is a slightly peralkaline crystal ash flow rhyolite tuff with about 10-15% phenocrysts of sanadine-anorthoclase with some biotite, clinopyroxene, and Fe-Ti oxides. Coatings are typically well developed and distinctively very dark chocolate brown to dark gray chocolate.

FELSIC TUFF AND PORPHYRY. Rhyolitic to latitic tuffs and lavas whose source is believed to be the Mount Helen caldera since unit proportions and probably thickness increase toward the volcanic center, occur over much of the Stonewall study area. A common sequence is dense quartz porphyry rhyolite lava capping friable poorly welded fine grained tuff with sparse to moderate lithic fragments. These units are very light in color - white to cream - with variable amounts of iron oxide stained coatings that are chiefly jarositic or limonitic in color and occasionally pastel reds and rouges. The lava sequence contains abundant medium grained quartz-eye phenocrysts, sanadine, and alkali feldspar. Angular breccia textures are present in places. This section seems to interfinger with ash flow sheets of Stonewall Flat Tuff. Coatings on the felsic rocks are immature and very poorly developed. They are cream to buff in color with rare patches of thin gray to very dark gray patina. The lavas are quite dense and tend to develop a thin (1-2mm) porcelanous rind in the immediate subsurface below the coatings. One of the more conspicuous features of the felsic deposits in outcrop is the presence of abundant rosettes of orange lichen. In places they cover outcrop and float to over 30% of volume and must add considerably to the spectral composition of their pixels. Another feature significant to remote sensing considerations is the presence typically of young shallow alluvial/eluvial rises covered with detritus weathered from adjacent felsic rock outcrop. These deposits form broad aprons with distinctive spectral properties.

BASALT. Basalt, probably derived from the Mount Helen caldera occurs at two sites in the Stonewall study area. Each is a relatively small exposure, but the unit is a stark contrast spectrally to surrounding cover in most images. The rock is very dark gray of the olivine basalt type, aphyric and vesicular. It forms thin gently dipping flows that lap the flanks of two felsic flow ridges.

BLACK MOUNTAIN CALDERA

The Black Mountain study area differs from Stonewall in two important ways: 1) the scene centers on a single well developed caldera with diverse flows produced by multiple caldera collapse and 2) more varied vegetative cover which influences spectral response. There are three mappable vegetative cover classes: sage brush and atropex dominate, foxtail and cheat grass dominate, and zones with low scrup juniper. Vegetation will be discussed in more detail below as it influences spectral response over individual units. Since some of the lavas at Black Mountain are indistinct in terms of coatings and imagery character, they are grouped together in the categories that follow. In general, however, units are described in order of decreasing age.

OLDER LAVAS AND TUFFS. Deposits of the Black Mountain Caldera overly older lavas and tuffs which occur principally in the western portion of the study area. These units are distinctive in composition and hand specimen. They are more silicic in general than rocks of the Black Mountain episode. The older lavas are leucocratic with coarse quartz and alkali feldspar phenocrysts. They tend to host more yellowish limonitic coatings and in places contain breccia textures.

CRYSTAL RICH LAVAS. Major extrusions of lava preceeded the ash flow sheets between each of the 3 or 4 caldera collapse events. They are from oldest to youngest, Lavas of Ribbon Cliff, Rocks of Yellow Cleft, and Lavas of Pillar Springs. Each unit is composed chiefly of trachyte. Lavas of Ribbon Cliff and Rocks of Yellow Cleft contain latites and syenites. The latites of Yellow Cleft are light in color with quartz and alkali feldspar phenocrysts. They are typically dense with breccia textures in places and contain very thin indistinct coatings. With the exception of the oldest unit, Ribbon Cliff, the deposits are peralkaline or trend toward peralkaline. Lavas of Ribbon Cliff and Pillar Springs are coarse crystal rich lavas which weather like granite. Phenocrysts are largely alkali feldspar with biotite and some quartz. Outcrops are rounded and exfoliated and occasionally form beehive mounds. Coatings are generally poorly to moderately developed and are dull brown to dull reddish brown in color.

TRAIL RIDGE TUFF. The Trail Ridge is the middle member of the Thirsty Canyon Tuff - the section of outflow sheets from the Black Mountain caldera. The unit occurs in a few small isolated patches in the study area. It overlies The Rocket Wash and Piute Mesa members, which are even represented less in the study

area and where they are present are indistinguishable in imagery from the lavas. The Trail Ridge member is a subalkaline rhyolite to quartz latite ash flow tuff. It tends to be moderately to densely welded in the study area. It is a brownish gray tuff with pumice fragments and alkali feldspar phenocrysts. Coatings are brownish to gray brown and darker and more maturely developed in general than those on the lavas.

GOLD FLAT TUFF. The Gold Flat Tuff is the uppermost ash flow sheet of the Thirsty Canyon Tuff and the most thoroughly studied formation in the project area. Noble (1965) identified the unit as pantellerite and a highly evolved iron enriched differentiate of the Black Mountain magmatic system. It's a thin moderately welded outflow sheet that caps mesas west and south of Black Mountain summit and the inner caldera rim. A thin basal vitrophyren separates it from Trail Ridge member. Lithologically the unit exhibits eutaxitic structure and contains 10-20% broken phenocrysts of quartz and sodic plagioclase with some clinopyroxene, amphibole, and olivene. Groundmass is devitrified to alkali feldspar and cristobalite. The Fe/Mg ratio of olivene and amphibole is high. Concentrations of Be, Nb, Pb, Sn, Th, and REE and anomalously high, up to 10 times that of typical comenditic glass from the Spearhead Tuff. Alkali/alumina and Na₂/K₂O ratios are unusually high as well. The unit is a distinctive very pale olive gray color in hand specimen. Coatings are gray brown to dark grayish chocolate and moderately well developed.

TRACHYTE OF HIDDEN CLIFF. After final collapse and extrusion of Gold Flat ash, mafic trachytic lavas filled the volcano and formed what is now the high edifice over Black Mountain. Mafic trachyte is dark gray, variably vesicular, largely aphyric with 5% plagioclase and alkali feldspar. The unit exhibits peralkaline trends geochemically. Outcrops on Black Mountain host about 10% dusty moss green to greenish gray lichen. Coatings are distinctively gray - light to medium - and moderately well developed.

LABYRINTH CANYON TUFF. The Labyrinth Canyon Tuff was recently recognized (Noble, et.al., 1984) as distal Spearhead Tuff of the Stonewall Flat Formation based on geochemical and paleomagnetic data. The thin somewhat platy ash flow is distinctive at Black Mountain. It is a very fine grained, very pale orangy buff comenditic rhyolite with sparse granule to pebble sized pumice fragments and alkali feldspar crystals. Basal vitrophyre separates it from underlying mafic trachyte lava. Coatings on the unit tend to be weak to moderately well developed and a pale orangy buff to dull gray brown color.

KANE SPRINGS WASH VOLCANIC CENTER

The units at Kane Springs Wash include several outflow sheets with distinctive chemistry, varying from subalkaline rhyolite to peralkaline iron enriched rhyolite (Noble, 1968). These units, however, apparently do not differ enough petrochemically to cause significant spectral variation. Rather imagery characteristics seem to depend more on coating development and perhaps vegetation as a function of degree of welding within individual sheets. Moreover differentiation is further achieved in the remote sensing data by identification of intra-sheet air fall tuff. The center is further unique among the 3 insofar as post caldera flows are abundant and confined to the intracaldera structure.

HICO FORMATION. The Kane Wash Tuff for the most part overlies an older felsic tuff. This pre-Kane Wash event deposit is a crystal rich ash flow. It weathers like exfoliated granite in places and forms mounds or beehive surfaces for landmark field recognition. It contains about 50% broken feldspar - sanadine-anorthoclase and plag., quartz, biotite, and amphibole. Pumice and other lithics are sparse. The unit contains variably welded zones alternating with less densely welded interzones. Coatings are more pronounced on dense weld portions of the tuff. They tend to be dull brown with variable tints of orange and gray, but mostly very pale orangy buff.

KANE WASH TUFF. In the study area the Kane Wash Tuff consists of 4 cooling units: a lowermost unit designated the "O" member, which overlies the Hico Formation; the "W" member which overlies the "O" member, then the "V1" and "V2" members as the section is ascended. Although earlier workers felt the "O" and "W" members were erupted from the Kane Springs center, Novak (1984, 1985), after conducting more detailed mapping believes they were sourced from a vent near the southern end of the Hico Range. All 4 of these members are similar in composition; however, since the older pre-Kane Wash eruption rocks tend to form a fairly coherent remote sensing unit, the Hico, "O", and "W" Tuffs are described as one unit in the imagery section that follows. Each unit contains phenocrysts of sanidine-anorthoclase, olivine (fayalitic), and pyroxene with some quartz. Sodic amphibole occurs in the vapor phase of the "V" members. Pumice fragments comprise about 5% of these outflow sheets. The "V" members are mostly densely welded but also strongly vapor phase altered. In places the less welded vapor phase altered zones are dense with lichen overgrowth.

"V2" is a comenditic rhyolite. These outflow sheets are separated by air fall deposits and basal vitrophyre. Coatings are quite well developed and a mature dark chocolate brown on densely welded layers. Less mature surfaces are an ashen gray brown.

AIR FALL TUFF. White, coarse, pumice rich to very fine lapilli tuff with rare pumice lithics occurs between the ash flow members of Kane Wash Tuff described above. A thick pumice rich white ash also occurs within the caldera apparently interfingering with the trachyandesite lavas. These rhyolitic pyroclastics are unwelded, nonresistent, vitric, white to cream colored, and quite conspicuous when coarse. Fine grained ash tends to be buff with pale orangy brown tints. Thicknesses vary from about 5 to 25 meters. Coatings are very poorly developed and seem be mostly transported dust and organic material.

CENTRAL SYENITE COMPLEX. After caldera collapse a roughly circular complex of extrusive to subvolcanic intrusive syenite erupted central to the caldera (Novak, 1984). The complex is texturally and compositionally diverse. The deposit is largely a fine grained cream colored porphyry with about 20% anorthoclase with clinopyroxene and up to 5% quartz. The unit forms a cumulodome approximately 5 km across that is resurgent into the caldera floor. It contains syenitic flow domes which resemble younger rhyolite flow domes described below. The lavas are massive and generally without flow layering. Coatings are tan to brown to reddish brown. Milky amorphous silica was noted in coatings on one of the flow domes.

TRACHYANDESITE LAVA. Dark gray, vesicular mafic trachyte forms elongate lava tongues about 100-150 meters thick in the western moat area. The unit was deposited during the post caldera collapse extrusive event. It contains about 15% phenocrysts of sieved plagioclase with olivene and clinopyroxene. The groundmass is holocrystalline and similar in mineralogy. Coatings are distinctly gray to rusty brown, usually dull, but occasionally dark with a manganese sheen. Coatings are sporadic but fairly well developed. They are lighter in color than coatings on basalt, but typically darker than coatings on the tuffs and rhyolites. The unit tends to host a relatively dense population of moss green to gray lichen similar to the lichen overgrowth on mafic trachyte of Black Mountain.

RHYOLITE DOMES. Flow layered rhyolite flow domes occur at two sites in the western caldera moat. These deposits are annular and appear exogenous over trachyandesite or intracaldera pyroclastics. They are a very pale flesh-tan color, quite dense and cap

prominent knolls which are thought to represent paleovent zones. Flow layering near the dome centers is subvertical. The white pumice rich pyroclastics which fill the western moat, probably erupted just prior to emplacement of these high silica rhyolite. The deposit contains phenocrysts of quartz, sanidine, plagioclase, fayalite, sodic amphibole, and Fe-Ti oxides. In a central lithophysal core, vapor phase topaz crystals up to 2mm long have been observed (Novak, 1984). Coatings on the rhyolite domes are chiefly pale orangy brown to moderately dark brown.

LATE BASALT. Late olivine basalt flows occur mostly capping mesa tops within the western moat area. They overly the white intracaldera pyroclastic deposit. Basalt also occurs in isolated patches outside of the caldera rim sourced apparently from several separate vents. Basalt is very dark gray and quite conspicuous in outcrop and talus scree. It is massive to vesicular. Coatings are gray to very dark and manganiferous.

IMAGERY CHARACTERISTICS

Imagery processing methods were described above. Only Landsat 5 Thematic Mapper data, bands 1, 2, 3, 4, 5, and 7, were investigated for this study. A multivariate statistical evaluation of pixel values for each scene was conducted with IDIMS function ISOCLS. A mean and standard deviation for each band and covariance matrix between bands were computed (Tables 4, 5, & 6). Correlation coefficients between bands is also given in Tables 4, 5, & 6. The matrix was derived by dividing covariance by the product of standard deviations of respective bands. The principle components transformation utilizes variance and covariance statistics. Resulting eigenvalues and eigenvectors are shown in Table 7. Eigenvalues are a measure of the amount of variance contained in each PC, thus the list compares variances contained between PC's.

In this section imagery characteristics of each major volcanic unit at each of the 3 study sites is evaluated with a view toward establishing effective imagery techniques and image combinations for formation discrimination and mapping. Studies so far indicate vegetation (only 25-30% of surface cover) is unimportant as a significant spectral control in the images at Stonewall.

STONEWALL MOUNTAIN AREA

SPEARHEAD TUFF. The Spearhead Tuff exhibits little spectral variation throughout the visible and near-IR. It is dark in all TM bands. Reflectivity decreases slightly and the unit darkens subtly in band 5 relative to other cover in the scene. Darker trends tend to increase the tonal contrast somewhat in 5/7 images, indicating reflectance rather than absorption in the clay absorption band. Intensity decreases slightly in the 3/1 ratio image; increases slightly in 5/1 images. These band relationships, of course, control color characteristics in false color composite images. So in 3/1-5/7-4 images, encoded RGB, the unit is magenta indicating higher reflectance in the 3/1 and 4 images with low reflectance in 5/7, and the unit is blueish gray in the 3-5-7 image (again RGB, respectively) due to higher reflectance in bands 3 and 7. In individual principle component images, the unit is brightest in PC3 with high brightness also in PC2 and PC4. Thus in the 3/1-5/7-PC2 composite the unit is a fairly distinctive dark purple. ISH computation on bands 3-5-7 result in indistinct low contrast tones over the unit in the saturation and hue modes, darker though in the

281.98
 187.56 130.57
 281.88 197.20 306.89
 220.05 154.54 241.63 194.74
 404.28 286.89 447.76 363.63 812.86
 189.81 135.00 211.03 172.99 402.59 222.75

 ESL IMAGE PROCESSING LABORATORY
 29-OCT-1986 23:15:49.37

 SUNNYVALE,

TOTAL NUMBER OF POINTS = 262144 ITERATION # 1

CLUSTER SYMBOL POINTS IN CLUSTER
 1 1 262144

MEANS

CLUSTER BND 1 BND 2 BND 3 BND 4 BND 5 BND 6
 1 162.74 81.15 117.54 97.43 165.83 99.75

STANDARD DEVIATIONS

CLUSTER BND 1 BND 2 BND 3 BND 4 BND 5 BND 6
 1 16.79 11.43 17.52 13.95 28.51 14.92

DISTANCES BETWEEN CLUSTERS

CLUSTER 1
 1 0.00

CORRELATION MATRIX (R)

1 1.00 2
 2 .98 1.00
 3 .96 .98 1.00
 4 .94 .97 .98 1.00
 5 .84 .88 .89 .92 1.00
 6 .76 .79 .81 .83 .95 1.00

$$R = \frac{\text{covariance}}{\text{stand. dev.} \times \text{stand. dev.}}$$

TABLE 4: Stonewall Mountain area image statistics

COVARIANCE MATRIX FOR CLUSTER 1

130.57					
79.23	51.37				
120.77	80.20	136.23			
88.18	61.04	109.05	100.12		
160.74	106.63	186.15	173.81	523.03	
112.54	73.97	123.71	107.46	353.06	260.27

 ESL IMAGE PROCESSING LABCRATORY
 4-NOV-1986 19:53:33.41

 SUNNYVALE,

TOTAL NUMBER OF POINTS = 262144 ITERATION # 1

CLUSTER	SYMBOL	POINTS IN CLUSTER
1	1	262144

CLUSTER	MEANS					
1	BND 1	BND 2	BND 3	BND 4	BND 5	BND 6
	129.04	61.00	87.69	78.38	146.99	89.85

CLUSTER	STANDARD DEVIATIONS					
1	BND 1	BND 2	BND 3	BND 4	BND 5	BND 6
	11.43	7.17	11.67	10.01	22.87	16.13

CLUSTER	DISTANCES BETWEEN CLUSTERS
1	0.00

CORRELATION MATRIX

1	1.00					
2	.97	1.00				
3	.90	.96	1.00			
4	.77	.85	.93	1.00		
5	.62	.65	.70	.76	1.00	
6	.61	.64	.65	.67	.96	1.00

TABLE 5: Black Mountain caldera image statistics

COVARIANCE MATRIX FOR CLUSTER 1

46

```

160.25
97.40   62.26
165.61 105.83 185.68
96.22   65.26 111.88 100.99
238.10 157.85 279.01 197.79 564.53
159.22 103.68 183.28 116.92 354.47 237.11

```

```

*****
ESL IMAGE PROCESSING LABORATORY
KS.SUB.6BANDS.STATS 6-MAR-1986 13:36:07.91
SUNNYVALE,CALI
*****

```

TOTAL NUMBER OF POINTS = 262144 ITERATION # 1

CLUSTER SYMBOL POINTS IN CLUSTER
1 1 262144

MEANS

CLUSTER	BND 1	BND 2	BND 3	BND 4	BND 5	BND 6
1	124.34	57.39	80.62	71.66	125.67	71.78

STANDARD DEVIATIONS

CLUSTER	BND 1	BND 2	BND 3	BND 4	BND 5	BND 6
1	12.66	7.89	13.63	10.05	23.76	15.40

DISTANCES BETWEEN CLUSTERS

CLUSTER	1
1	0.00

CORRELATION MATRIX

1	1.00					
2	.96	1.00				
3	.96	.98	1.00			
4	.76	.82	.82	1.00		
5	.79	.84	.86	.83	1.00	
6	.82	.85	.87	.76	.97	1.00

TABLE 6: Kane Springs volcanic center image statistics

I EIGENVALUE(I)

1 1797.656250
 2 118.011215
 3 17.116089
 4 12.925664
 5 2.660455
 6 1.412745

TABLE 7: Principle components statistics

ORIGINAL PRICE IN
 OF POOR QUALITY

TRANSFORMATION MATRIX (EIGENVECTORS)

Stonewall Mountain

0.368303	0.257569	0.398771	0.319566	0.657626	0.323108
-0.506020	-0.285845	-0.380288	-0.223752	0.512003	0.453217
0.518041	0.058601	-0.241535	-0.287526	-0.359411	0.676766
0.488046	0.004007	-0.404738	-0.436638	0.419167	-0.481278
0.277976	-0.571174	-0.382229	0.670561	-0.014871	-0.022747
-0.156429	0.722676	-0.572811	0.353322	-0.016803	-0.006083

I EIGENVALUE(I)

1 1005.116760
 2 151.754028
 3 31.079649
 4 10.118806
 5 2.476775
 6 1.044413

Black Mountain

TRANSFORMATION MATRIX (EIGENVECTORS)

0.276864	0.181794	0.307719	0.268180	0.701000	0.481959
0.529437	0.329714	0.498072	0.303647	-0.404013	-0.327843
-0.531388	-0.157900	0.179655	0.634960	0.237252	-0.448281
-0.436464	0.030353	0.352061	0.178230	-0.496493	0.637464
-0.269929	0.041677	0.661288	-0.632469	0.198914	-0.220261
-0.311942	0.911400	-0.252405	-0.030350	0.054876	-0.056354

I EIGENVALUE(I)

1 1185.295044
 2 81.124763
 3 32.253185
 4 6.022783
 5 5.215764
 6 0.892326

Kane Springs

TRANSFORMATION MATRIX (EIGENVECTORS)

0.328391	0.213222	0.373145	0.250498	0.675531	0.434013
0.595729	0.305867	0.464812	0.085820	-0.519128	-0.242165
-0.191788	-0.002714	-0.058222	0.883454	0.067267	-0.418096
-0.300434	0.010174	0.124051	0.325236	-0.512271	0.725291
0.596664	-0.057100	-0.737487	0.194919	-0.083320	0.227836
-0.232841	0.926073	-0.286440	-0.074986	0.016611	-0.015000

intensity image. This results in a distinctive dull army green hue for the image in the ISH composite. Indeed, basalt exposures, shadows, and the ash flow units with their dark desert varnish coatings tend to register high DN values in the saturation mode. Relationships are similar on ISH images of bands 1-2-4, thus a hue composite of bands 1-2-4 with scaled bands 3 and 7 results in distinctive blueish hues over the unit; green if intensity is used instead of hue in the same configuration.

CIVET CAT CANYON TUFF. Reflectance over Civet Cat is low in bands 1, 2, and 3 and high in bands 4, 5, and 7, increasingly so in the later 3 relative to other cover in the scene. These spectral relationships cause the unit to be subdued in 3/1 and 5/7 ratio images, but strikingly bright in the 5/1 ratio image. High scene reflectance in band 7 creates high contrast turquoise blue over the unit in 3-5-7 images. The unit registers a dull, indistinct pale grayish green in the 3/1-5/7-4 image. There is a low intensity but high saturation and hue response for the unit in ISH computations with bands 3-5-7, resulting in a distinctive moss green contrast in the composite ISH image. On ISH images with bands 1-2-4 the unit shows low values in intensity and hue, high values in saturation, but low contrast in all three modes. Civet Cat is strikingly bright in PC2 images, growing somewhat less so in PC's 3 and 4. This results in impressive discrimination capacity over the unit in the PC2-PC3-PC4 and PC2-PC4-PC5 images in which the unit is a high contrast icy peach. The unit is also rather anomalous in contrast on some of the more exotic composites, including especially a 1-4-Hue image, Hue computed on bands 3-5-7; the 3/1-5/7-PC2 image, and a 3-7-Hue (bands 1-2-4) composite. A 3/1-PC2-Hue (bands 3-5-7) is especially effective in highlighting the Stonewall Flat Tuff in general.

FELSIC TUFF AND PORPHYRY. With respect to remote sensing traits, the felsic units differ from the ash flow deposits described above not only compositionally but also in manner of distribution. The felsic deposits form broad alluvial/eluvial fans down gradient that are spectrally largely indistinguishable from outcrop. The unit exhibits high reflectivity in all bands with diminishing intensity in longer wavelength bands 5 and 7. Band ratios tend to dampen intensities relative to other cover or enhance differences in iron oxide coatings and clay altered surfaces. For example, several exposures are quite bright in 5/7 ratio images. The unit contrasts markedly with other formations in most color composite images. On 3-5-7 and 3/1-5/7-4 images the units is cream colored and iron oxide stained areas reddish to red brown. On the ISH computations, bands 3-5-7, the unit is bright in

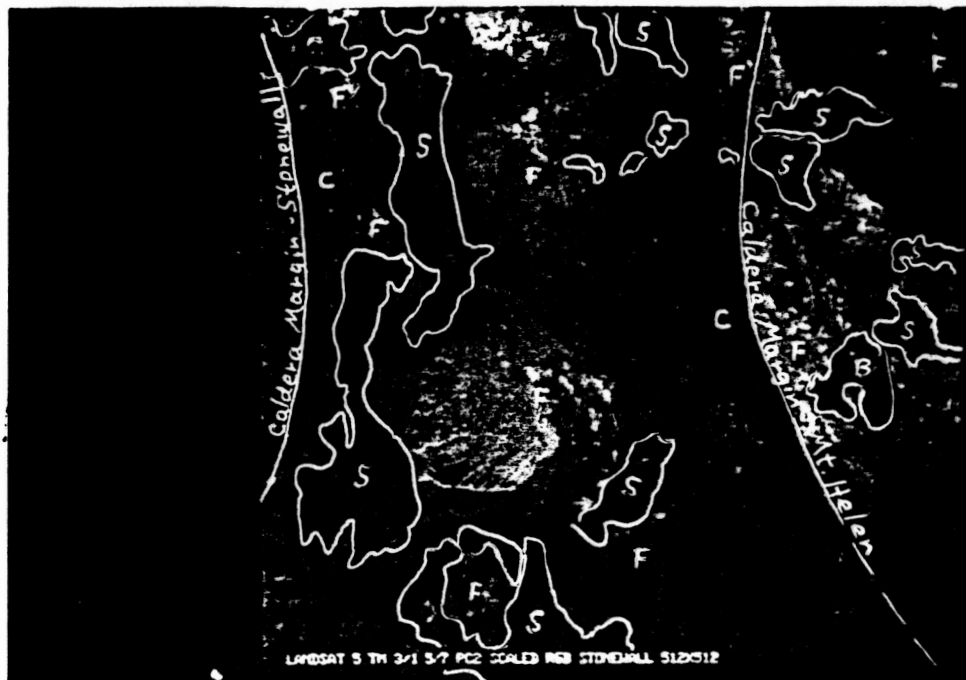


FIGURE 14. Stonewall Mountain TM image. Band ratios 3/1 and 5/7 combined with PC2 in a false color composite encoded red, green, and blue, respectively. All bands stretched by scaling. S - Stonewall Flat Tuff, B - basalt, C - quartzite conglomerate, unconsolidated, F - felsic tuffs and flows.

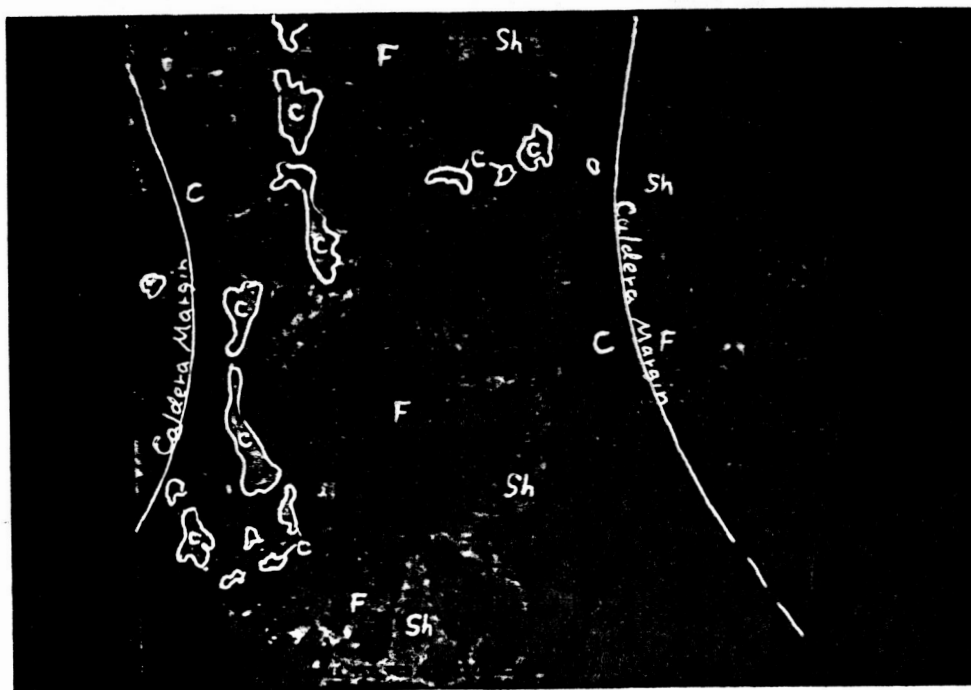


FIGURE 15. Stonewall Mountain area TM image. False color composite of PC's 2, 3, and 4, color encoded red, green, blue, respectively. All PC's scaled. C - Civet Cat Canyon Member of Stonewall Flat Tuff, Sh - Spearhead Member, C - quartzite conglomerate, unconsolidated, F - felsic tuffs and lavas.

ORIGINAL PAGE IS
OF POOR QUALITY

saturation and intensity, light to medium gray in hue. In 1-2-4 ISH renditions the deposit is quite dark in hue and saturation, light in the intensity mode. These felsic rocks respond with bright intensity in PC1, dark and indistinct in PC2, and with only slight variation in higher PC's. Thus PC1 overpowers other bands in composites in which it is included and PC composites without PC1 tend to obscure these units. In the 3/1-5/7-PC2 image they are brightly yellow to reddish and quite conspicuous. Perhaps the greatest overall contrast over the unit is exhibited by the 3-7-Hue (bands 1-2-4) image in which it is highlighted in bright yellow and the 3-5-7 ISH composite in which it is bright red.

BASALT. Basalt is dark in all bands, decreasing slightly in brightness in longer wavelength bands 5 and 7. It is thus medium gray and obscure in the 5/7 image and not appreciably changed by 3/1 and 5/1 ratios. On the 3/1-5/7-4 composite basalt is swamp green and well highlighted. It is dark brown on the 3-5-7 composite. In the individual modes of the 3-5-7 ISH transformation, the unit is dark; however, on the 1-2-4 ISH saturation and hue images it is very bright. Thus on the 3-7-Hue (bands 1-2-4) composite basalt is purple and on the 3-5-7 ISH composite, greenish. It is very dark in PC1, obscure and indistinguishable in PC2, slightly brighter in PC's 3 and 4. It is highlighted, therefore, by blue in the PC1 PC2 PC4 composite, but cannot be discriminated on the PC2 PC4 PC5 image. On the 3/1-5/7-PC2 image the unit is a deep, rich green.

BLACK MOUNTAIN CALDERA

Imagery over the Black Mountain study area differs from Stonewall primarily as a function of more diverse vegetative cover. Lithologies are more varied as well. Still the outflow sheets tend to be readily mappable with Landsat TM imagery. Vegetation has been described above. The 4/3 ratio image highlights zones with relatively heavy growth. This image is matched very closely by the PC3 image which also presents vegetation in strikingly bright contrast.

OLDER LAVAS AND TUFFS. The older felsic lavas and tuffs are the most reflectant cover in lower wavelength bands - 1-4. They are intermediate in reflectance at higher wavelengths. In the ratioed images the unit tends to be dull, intermediate in intensity and indistinct. Some parts of the unit, however, exhibit a brighter signature in the 3/1 image due to iron oxide staining. Alluvial material and drainages down slope of these areas are also bright. The deposit is a distinctive rusty cream color on the 3-5-7 composite.

ORIGINAL PAGE IS
OF POOR QUALITY

It is bright on both the PC1 and PC2 images and therefore exhibits a yellow signature on composites combining PC's 1 and 2, a reddish color if only one of them is in combination with other variables and it is encoded red. In the 5-7-PC2 composite the unit is a pastel purple due to high DN values in 5 and PC2 and low DN values in band 7. With ISH transform on bands 3-5-7 the unit is quite bright in the intensity mode relative to other cover, bright in saturation, but only medium in hue. Thus a distinctive yellow color over these rocks in the 1-4-Hue composite. (Hue is subdued for this formation.)

CRYSTAL RICH LAVAS. The intra-ash flow lava flows at Black Mountain, exclusive of Trachyte of Hidden Cliff, form a generally coherent remote sensing unit at Black Mountain. The lavas are dark in all bands, growing slightly darker with increasing wavelength. Lavas of Ribbon Cliff seem to be slightly darker than the others in bands 5 and 7. The units tend to be light to medium-light gray and indistinct in the ratio images. In the color composite 3/1-5/7-4 image the lavas are yellowish green and basically indistinguishable from Trachyte of Hidden Cliff. On the 3-5-7 image, however, they are a greenish brown. Lavas of Ribbon Cliff are more reddish than the other lavas on this image possibly reflecting a higher proportion of brighter iron oxides in the coatings. This distinction is mirrored on the 1-4-Hue (bands 3-5-7) image. On the 3-5-7 band ISH images, the lavas are dark in saturation and hue, indistinctive medium gray in the intensity mode. In the principle components transformation lavas are brightest relative to other cover in PC2, the PC4, dark in PC1. So in the PC composites, PC2 controls their contrast and in composite PC1 PC2 PC3 they are greenish, and in PC2 PC3 PC4, reddish. They contrast in the later with Trachyte of Hidden Cliff which is emerald green probably due to the vegetative response of the summit area of Black Mountain.

TRAIL RIDGE TUFF. The Trail Ridge Tuff is relatively bright in all bands. It tends toward slightly darker in higher wavelengths but against its usual background of lavas, which also grow slightly darker, it appears bright. It is indistinct on ratio images as well as single band and hybrid color ratio composites and requires more advanced transformations and enhancement techniques to identify. The unit is light in PC1, less so in PC2, growing darker and more difficult to identify in higher PC's. It tends to be orangy or golden in color in PC composites that include PC1 and PC2, or either of these PC's. In the ISH transformation with bands 3-5-7 Trail Ridge is quite bright in saturation and hue, less so in the intensity mode. In

most color composites that include an ISH parameter the unit is indistinguishable from other ash flow deposits; however, it is a paler avocado green on the 3-5-Hue (bands 1-2-4) image and a unique pinkish buff in the 1-4-Hue (bands 3-5-7) image.

GOLD FLAT TUFF. The Gold Flat Tuff is an unusual rock petrochemically and is distinctive spectrally as well. Reflectance increases as wavelength increases to brightest in band 7. For this reason distinctly dark in the 5/7 image and reddish to magenta in 3/1-5/7-4 false color composites. The unusually high reflectance in band 7 relative to other scene cover gives rise to a strikingly bright turquoise blue hue in the 3-5-7 composite. Gold Flat Tuff is bright in PC1, very dark and anomalous in PC2, and dark as well in PC3 except over its northern exposures where it is masked by the bright response of vegetation. It is medium gray, indistinct in PC's 4, 5 and 6. This relationship among eigenvalues results in reddish hues over the formation in composites involving PC1 and bluish to purplish hues in the PC2 PC3 PC4 composite. The unit is intensely bright in saturation and hue images with ISH transformation on bands 3-5-7, medium in intensity in the intensity mode. On the ISH false color composite the unit is a very distinctive pale powder magenta. On the 5-7-PC2 composite, Gold Flat is a brilliant mustard yellow, but so is Labyrinth Canyon Tuff. It's light purple in the 1-4-Hue (bands 3-5-7), blue where vegetation includes golden grasses and scattered low juniper.

TRACHYTE OF HIDDEN CLIFF. Mafic trachyte forms the central volcanic edifice and is very dark in all bands except 4 and 5 in which it is an indistinct medium gray. Spectral response appears to be influenced by vegetation, which in this case would be golden cheat grasses and lichen. The unit is very bright relative to anything else in the scene in the 5/7 and 4/3 images in a slightly striped pattern that apparently follows drainages and is probably caused by high vegetative reflectances in bands 4 and 7. In individual PC's the deposit is quite dark in the first PC, very light due to vegetative interference in the third. Mafic trachyte is a pinkish purple on the PC1 PC2 PC3 composite, yellowish green in the PC2 PC3 PC4 rendition. It is indistinct from other lavas in the PC2 PC4 PC5 image, due apparently to absence of a parameter responsive to vegetative reflectance. In the ISH transform of bands 3-5-7, the unit is very dark in intensity and hue, medium gray and indistinct in saturation. On the ISH composite it is purplish. In the 1-4-Hue (bands 3-5-7) image, mafic trachyte is dark forest green and a dull army green on the 3-5-hue (bands 1-2-4) image.

LABYRINTH CANYON TUFF. The Labyrinth Canyon ash flow tuff, really a distal facies of Spearhead Tuff, is spectrally similar to Gold Flat Tuff. It tends to be moderately to only slightly bright in bands 1-3, quite bright in bands 4 and 5, somewhat less so in band 7. It is slightly less reflectant in band 7 than Gold Flat which aids its discrimination in false color composite images which take this relationship into account. It is bright in the 3/1 image, possibly due to its orangy buff color, and medium gray with 5/7 ratios, but much lighter in tone from the Gold Flat Tuff. Labyrinth Canyon is a pale powder blue and distinct from Gold Flat in the 3-5-7 composite and unique in color contrast as well in 3/1-5/7-4 hybrids in which it is a very pale pink. The unit is bright in PC1, dark in PC2. It appears masked by the bright vegetative response of cheat grass in PC3. It is pale pinkish lavender on the PC1 PC2 PC3 composite, a bright orangy red on the PC1 PC2 PC4 configuration. Saturation and hue images of bands 3-5-7 give the unit a very bright signature, less so in the intensity mode. The deposit occurs with fair color contrast as well in the 1-4-Hue (bands 3-5-7) and the 3-5-Hue (bands 1-2-4) composites. Color is not unique for the unit on the PC2 composites with bands 5 and 7 and bands 3 and 7.

KANE SPRINGS WASH VOLCANIC CENTER

Imagery response of units at Kane Springs Wash is influenced much more strongly by topography and vegetation than the other 2 study sites. Topographic relief is almost 1000 meters and juniper trees dot the mesa tops, particularly in the northern part of the caldera. Other vegetative cover is also thicker throughout the scene at Kane Springs Wash, including foxtail grass, cheat grass, atroplex, sage brush, boxbrush, and cactus plants.

PRE-KANE WASH EVENT TUFFS. The older, pre-Kane Wash volcanism, tuffs occur as a single remote sensing unit. The Hico Formation and "W" tuff are relatively thin in horizontal exposure, the later especially so due to its dense weld cliff forming nature. Therefore, imagery response is dominated by the "O" tuff. Reflectance off the older tuffs - Hico, "O", and "W" - increases in intensity in higher wavelength bands. The unit as a whole is characterized by a banded pattern (mostly in the "O" Tuff) of alternating reflectivities due to successions of repetitious vapor phase and dense weld stratigraphy. The unit is brighter in 3/1 and 5/2 ratio images, darker with a 5/7. It is indistinct in simple color composites and hybrid composites. The deposit is bright in PC1, obscure in other PC's. In the ISH transform, bands 3-5-7, the section is relatively

bright in the intensity mode, medium gray in hue and saturation. Complex color composites tend to highlight the interval best. In PC1 PC2 PC3 and PC1 PC2 PC4 composites the formation is characterized by a reddish banded image. It's a faded powder blue in the 1-4-Intensity (ISH, bands 3-5-7) image and reflects a subtle distinction in other ISH hybrids with other bands. For example, a 3-7-Saturation (bands 2-4-5). the 3-5-7 ISH Intensity parameter image exhibits the unit with relatively bright intensities.

KANE WASH TUFF UNITS V1 AND V2. The Kane Wash event tuffs exhibit medium gray tones in lower wavelength bands, but are relatively bright in band 5, increasingly so in band 7. The unit is quite bright in the 5/1 and 5/2 ratio images, rather dark in the 5/7 image. In the 3-5-7 composite the section is a distinctive powder blue. It is an indistinct red in the 3/1-5/7-4 image. The tuffs are extremely bright in the Hue mode of the 3-5-7 ISH transformation; dark in saturation; and medium gray in the intensity mode. Its a reasonably distinctive lavender in the ISH composite. In PC1 the unit is medium gray; in PC2 quite dark where densely welded; then relatively light in PC's 3-5. In composite PC's - 1-2-3 and 2-3-4 - the formation is distinct, especially the later within which it tends to be bright blue. In more exotic renditions with ISH and simple band hybrids the section is typically highlighted with some characteristic tint. This appears to be due primarily to the presence of large areal exposures of densely welded zones.

AIR FALL TUFFS. The air fall tuffs which tend to be very light in color are highly reflective in all wavelengths. This characteristic controls the units response in false color composite images. These tuffs are quite bright in PC1 and uniquely so in PC2. Tonal contrast is obscure in further PC's. In all ISH transformations these glassy beds are bright in intensity mode, obscure in saturation and hue. The deposits are more uniquely highlighted by PC composites and the 1-4-Saturation (bands 3-5-7) image.

SYENITE COMPLEX. The syenite complex is recognizable on images only as an anomalous textural pattern in tonal and color variation over a generally circular zone. The pattern is created by irregular reflectance properties over relatively small areas throughout the complex. Reflectance is variable, but more consistently bright in the higher wavelength bands. In individual PC images the unit exhibits overall medium intensity brightness except in PC2 in which it is relatively dark. The subtly distinct busy textural pattern seems fairly equally highlighted in complex composites with highly variable hues and tints.

TRACHYANDESITE LAVAS. The trachyandesite lavas are exposed primarily in the canyons within the caldera complex. They are thus largely obscured by shadow and tend to blend with shadows. The unit is relatively nonreflectant and dark in all bands. It is relatively light in the 5/7 image due to slightly higher reflectivity in band 5. The deposit is light in tone in PC2, dark in all other PC's. The formation is anomalously dark in the hue mode of the 3-5-7 ISH transform and bright in saturation. Its a reddish brown to greenish brown color in the 1-4-Hue (bands 3-5-7) image and the 1-4-Intensity image.

RHYOLITE FLOW DOMES. The rhyolite flow domes and syenite domes of the syenite complex exhibit very similar image signatures. This description of rhyolite can be applied as well to the syenite domes. Part of the discriminatory capability of these units is a function of their concise small circular outline. Tonal contrast and color patterns within them is highly varied. So in that regard they behave similarly to the syenite complex described above. The rhyolite and syenite flow domes are highly reflective in all bands, but more so in band 7. For that reason rhyolite domes form strikingly anomalous dark bullseye contrasts in the 5/7 ratio image. It is a brilliant red color in the 3/1-5/7-4 composite. The formation is uniquely bright in PC5, quite bright also in PC1. It is darker in PC2. The unit tends to mirror the tuffs in all composite images. It exhibits slight deviation from the tuffs, however, in the 1-4-Saturation or Intensity (bands 3-5-7) composites. Recognition is dependent in part on the near circular outlines of the domes. Perhaps the best images for its discrimination are the individual bands, PC5, 5/7 ratio, and saturation of bands 3-5-7 in which the unit is dark.

LATE BASALT. Basalt primarily caps the mesas within the caldera and its Landsat spectra are contaminated with a significant contribution from vegetation including sparse to moderately dense juniper. The basalt flows are dark in all bands, slightly more reflective in band 5. They are rather light, however in the 5/7 ratio image and therefore greenish on the 3/1-5/7-4 composite. In the 3-5-7 composite the lavas are blue to greenish. The unit is very dark in PC1, indistinct in other PC's. On the PC composites, 1-2-3 and 2-3-4, basalt is dark blue to dusty blue. On the intensity image of the ISH function on bands 3-5-7 the formation is dark. It is indistinct in hue and saturation. On the 1-4-ISH composites the unit is a dark felty green. Basalt is a rather distinctive purple on a 3/1-5-PC2 image.

COATINGS ON ROCKS IN THE PROJECT AREAS

Coatings on the volcanic rocks at Stonewall Mountain, Black Mountain, and Kane Springs Wash are typical of weathered surfaces on rocks throughout the semi-arid West and Southwest, U.S. Descriptions of coatings in general and details of analytical investigations by other workers in similar environments were presented in an earlier section. This section describes macroscopic, microscopic, and X-ray diffraction characteristics of coating samples from the 3 project areas.

Analytical methods were described in an earlier section. So far over 50 thin sections have been studied to varying degrees of detail, but basically in a preliminary fashion. And X-ray diffraction analysis of 52 surface coating samples was accomplished. The results of this work are incorporated in the discussion of coatings that follows.

The nature of coatings varies with underlying host rock in a manner correlative with host petrochemistry, degree of welding, devitrification, hyalinity, porosity, and other textural and physiochemical properties. Coatings may vary consistently enough from one formation to another to differentiate units in the field, inferentially.

A paragenetic zonal relationship occurs within the altered weathered zone of the volcanic units. The nature of secondary products on any given exposure is dependent on the degree of maturation of weathering which depends directly on host rock density and resistance to mechanical degradation. The arid surface interface of the units contains the desert varnish. Varnish is only about 0.1mm thick and stains the surface as a coating which impregnates slightly (less than 0.1mm) along mineral boundaries much as an enamel paint might. Thin section observation and X-ray diffraction analyses show the varnish is noncrystalline. It appears to be an amorphous hematitic product (Figures 18 and 19). Two samples of coatings from older tuffs of Kane Springs registered a 2 theta peak near a 2d spacing for the clay mineral illite, but lacked most peaks characteristic of illite at other 2d spacings. The sample was run on the school's new Phillips XRG 3100 computerized XRD and compared with it's disc powder file library. The only realistic mineral selected was a hydrous silicate - $\text{H}_2\text{Si}_2\text{O}_5\text{H}_2\text{O}$. It is likely the mineral is either a poorly ordered mixed-layer illitic clay or perhaps this hydrous silicate. Kaolinite is apparently present in coatings from two samples from Stonewall Mountain - rhyolite and Andesite from the Mount Helen caldera. No clays registered from coatings on the ash flow units. The dominate minerals present in the samples (see following



FIGURE 18. Photomicrograph of basalt from the Stonewall Mountain area, showing reddish brown coating. Crossed nichols, 2.5 power.

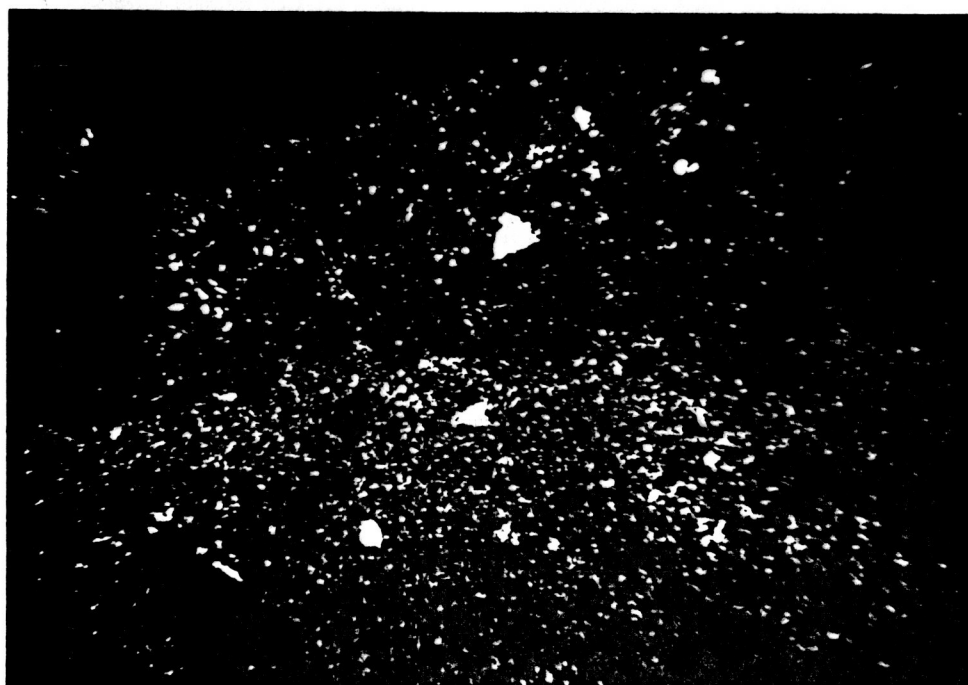


FIGURE 19. Photomicrograph of Spearhead Tuff Member from the Stonewall Mountain area, showing siliceous rind with thin faint reddish desert varnish coating at the top and fine. Crossed nichols, 2.5 power.

table) and represented by characteristic 2 theta peaks include quartz, alkali feldspar, probably sanadine and anorthoclase (potassian albite), and more calcian plagioclase. These are primary minerals derived from the substrate beneath the varnishes. Analcime was detected in the coating sample from a minor air fall tuff unit at Stonewall.

On resistant units such as basalt or densely welded tuff varnish will be longerlived and relatively mature. It tends to be darker - browns and grays - relative to varnishes on less resistant units. Compositions appear to be dominated by iron and manganese oxides which would be consistent with analytical work on similar rocks by other workers. Varnishes on basalts, mafic trachytes and other mafic units are darker on average and presumably enriched in manganese relative to iron. Indeed, if the darker varnishes do contain proportionally higher manganese, the relationship would support observations by other workers that manganese is preferentially enriched in varnishes with time. As was noted earlier, they do occur on the most long lived surfaces. These darker varnish varieties also tends to be more consistent and pervasive when present, whereas exposures of poorly welded tuff, vapor phase altered tuff, and other less consolidated rocks are more a mix of coatings, subsurface weathered rinds, and relatively fresh rock. Also, the softer formations seem to provide better foundations for lichen which further diversifies the surface and complicates the spectral characteristics and aerospace imagery.

Varnishes tend to ride a case hardened zone that exfoliates the surfaces of the volcanics. This thin .3-.8mm rind spalls off the outcrops exposing a substrate with secondary alteration characteristics as well. The subsurface altered zone beneath the hardened shield is generally light in color - cream, buff, or orangy buff, stained apparently with limonitic iron oxides - on the ash flow tuff units. The zone is largely absent in most lavas and vitric tuffs, particularly the basalts and mafic trachytes. Thin section observation reveals the zone is comprised of a very fine grained mesh of apparently secondary minerals possibly clay or sericite. This material has not yet been studied in detail. In some of the sections this zone diminishes in alteration intensity gradually beyond about .6mm within the host. On the lavas, varnish tends to ride stain-like atop fresh relatively unaltered primary minerals. In case hardened zone overlying the argillic zone, clay minerals are absent. The case hardened shells are apparently enriched in quartz, possibly as a primary phenomenon related to cooling. These zones will be studied in considerably more detail in the coming months.

COATING SAMPLES ANALYZED BY X-RAY DIFFRACTION

Sample	Minerals Detected
Stonewall Mtn	
44 felsic tuff	Q, AF
42 Civet Cat Tuff	Q, AF
50 Stonewall Tuff	Q, AF
51 rhyolite Q por	Q, AF
12 basalt	AF
30 Spearhead Tuff	Q, AF
13 air fall tuff	Q, AF, Analcime
20 Spearhead Tuff	Q, AF
31 divitrified glass	Q, AF
34 rhyolite Q por	Q, AF
37 rhyolite Q por	Q, AF, Kaolinite
39 andesite por	Q, AF, Kaolinite
33 vitric ash	Glass
32 vitrophyre	Glass, Minor Q, AF
Black Mtn	
57 Trail Ridge Tuff	Q, AF
59 Gold Flat Tuff	Q, AF
58 crystal lava	Q, AF
61 Divitrified glass	Q, AF
56 crystal lava	Q, AF
22 Trail Ridge Tuff	Q, AF
11 trachyte	AF
62 alluvial gravel	Q, AF
25 Gold Flat Tuff	Q, AF
16 Labyrinth Tuff Q,	AF
60 Gold Flat Tuff	Q, AF
21 divitrified glass	Q, AF
24 Rocket Wash Tuff	Q, AF
20 Gold Flat Tuff	Q, AF
23 Trail Ridge Tuff	Q, AF
15 basal vitrophyre	Glass
27 Trail Ridge Tuff	Q, AF
10 Trail Ridge Tuff	AF
40 trachyte	Q, AF
55 crystal lava	Q, AF
Kane Springs	
52 Kane Wash Tuff	Q, AF
48 Kane Wash Tuff	Q, AF
47 Kane Wash Tuff	Q, AF
49 Kane Wash Tuff	Q, AF
56 Kane Wash Tuff	Q, AF
54 Kane Wash Tuff	Q, AF
53 Kane Wash Tuff	Q, AF
24 syenite dome	Q, AF
8 trachyandesite	AF
10 rhyolite dome	Q, AF
21 basalt	AF

11 trachyandesite	AF
53 Kane Wash Tuff	AF
38 Hico ash flow	Q, AF, Illite(?)
40 Kane Wash Tuff	Q, AF
26 trachytic ash	Q, AF
4 vitric tuff	Glass, minor Q
39 pumice air fall	Q, AF, Illite(?)

Q - Quartz, AF - Alkali Feldspar, mostly sanadine
and anorthoclase (potassian albite)

CONCLUSION

IMAGERY

Preliminary results of imagery processing analysis at the 3 project sites indicate that TM data is quite effective at discriminating certain volcanic lithologies. In general volcanic lavas and ash flow units exhibit characteristic spectra in the visible and near-IR as a function of iron content or felsic index. Vegetation at Black Mountain and Stonewall Mountain, although detectable and certainly a contributing spectral factor seems overwhelmed by the spectral contribution of lithologies. This relationship is less distinct at Kane Springs Wash, due possibly to topographic and vegetative effects, both of which are more extreme an influence at this project site.

The origin of the distinctive spectral character of these volcanic lithologies is one of the chief pursuits of this project. Much more data will be collected before conclusions are drawn; however, it appears at this time that features inherent to primary petrochemical and textural relationships are a major control. The extent to which coatings are influencing the spectra seems apparent in some instances (dark red bands of dark, mature, coating encrusted, dense weld zones in tuffs at Kane Springs Wash in the PC1 PC2 PC3 composite, for example), but the degree to which coating types are classifiable independently of underlying host lithologies seems greatly subordinated to the latter.

The discriminating ability of TM data originates from the fact that relatively felsic rocks are more reflectant than mafic rocks in all wavelengths of the TM range (excluding the thermal band). This relationship is enhanceable with computer processing functions which increase contrast between lithologies and presents them in striking color classification schemes. Since all rocks in arid/semi-arid environments develop secondary mineral coatings to some degree, it seems reasonable that coating character might reflect underlying host composition in a way that significantly influences spectral properties. This question is the focus of present research.

Lithologic differentiation of volcanic rocks in southern Nevada seems best achieved with color composite images of bands 3, 5, and 7. The longer wavelength bands discriminate cover better than the shorter ones for most cover types. Enhancement techniques including band ratios, ISH transforms, and principle components analysis provide even further

contrast and when combined in composite color images in relationships derived through trial and error processing experimentation, these spectral differences are enhanced markedly. The following composite images seem best for overall rock discrimination (all bands contrast enhanced by linear stretch).

Bands 3 5 7
 ISH bands 3 5 7
 PC1 PC2 PC3
 PC2 PC3 PC4
 PC2 PC4 PC5
 3/1 5/7 PC2
 3/1 5/7 Hue or Satur. on bands 1 2 4
 3 5 Hue or Satur. on bands 2 4 7

COATINGS

Coatings include true desert varnish, an extremely thin 0.1mm air interface, cooling rinds on ash flows, and weathered or oxidized zones. Coatings are basically any secondary (including diagenetic) surface which essentially shields primary host lithologies. X-ray analysis of varnishes and the very shallow subsurface beneath varnishes (0.5mm thicknesses) indicates that amorphous probably iron and manganese enriched material is the chief component. Clay minerals do not appear to be important in the varnish zone.

Lavas tend to support films of desert varnish in direct contact with fresh feldspar and quartz. Ash flow tuffs tend to develop rinds of silica rich deposits probably formed after deposition but during the cooling phase (Ross, 1961). These rinds have been observed on rocks of the project areas and appear to be unaltered silicic zones, but the exact nature of these features is under analytical review at this time.

This is an interim report. This NASA funded project will continue into 1988. Current efforts are on analyses of coatings and rinds and weathered rock surfaces, improved enhancement techniques, and more quantified approaches to image classification.

REFERENCES

- Abrams, M.J., Ashley, R.P., Rowan, L.C., Goetz, A.F.H., and Kahle, A.B., 1977, Mapping of hydrothermal alteration in the Cuprite mining district, Nevada, using aircraft scanner images for the spectral region 0.46 to 2.36: *Geology*, v.5, p.713-718.
- Allen, C.C., 1978, Desert varnish of the Sonoran Desert: optical and electron probe microanalyses: *Jour. of Geol.*, v.86, p. 743-752.
- Baird, A.K., 1984a, Iron variation within a granitic pluton as determined by near-IR reflectance: *Jour.Geol.*, 92, p344-350.
- Baird, A.K., 1984b, Granitic terranes viewed remotely by shuttle IR radiometry: *Jour.Geoph.Res.*, v.89, B11, p9439-9447.
- Berner, R.A., and Holdren, G.R., Jr., 1977, Mechanism of feldspar weathering: some observational evidence: *Geology*, v.5, p.369-372.
- Borengasser, M.X., Brandshaft, D.R., and Taranik, J.V., 1984, Geological application of enhanced Landsat 4 TM imagery of south central Nevada: *Int. Symp. on Remote Sensing of Envir., Third Thematic Conf., Remote Sensing for Explor. Geol., Colorado Springs, Colo.*, 8 p.
- Borns, D.J., Adams, J.B., Curtiss, B., Farr, T., Palmer, F., Staley, J., and Taylor-George, S., 1980, The role of micro-organisms in the formation of desert varnish and other rock coatings: SEM study: *GSA Abst.*, v.12, p.390.
- Byers, F.M., et.al., 1976, Volcanic suites and related cauldrons of Timber Mountain - Oasis Valley caldera complex, southern Nevada: *U.S.G.S. Prof.Paper 919*, 70p.
- Buchanan, M.D., 1979, Effective utilization of color in multidimensional data presentations: *SPIE*, v.199, p.9-18.
- Clark, S.P., 1957, Absorption spectra of some silicates in the visible and near infrared: *Amer. Mineralogist*, v.42, p.732-741.
- Cook, E.F., 1965, Stratigraphy of Tertiary volcanic rocks in eastern Nevada: *Nev. Bur. Mines Rept. No. 11*, 61 p.
- Cornwall, H.R., 1972, Geology and mineral deposits of southern Nye County, Nev.: *Nev.Bur.Mines and Geol.*

Bull. 77. 49 p.

Curtiss, B., Adams, J.B., and Ghiorso, M.S., 1985, Origin, development and chemistry of silica-alumina rock coatings from the semi-arid region of the Island of Hawaii: *Geoch. Et Cosmo Chem. Acta*, Jan. vol.

Davis, J.C., 1973, *Statistics and data analysis in geology*: John Wiley & Sons, N.Y., N.Y., 2nd edit., 550p.

Dorn, R.I. and Oberlander, T.M., 1981, Microbial origin of desert varnish: *Science*, v. 213, p. 1245-1247.

Dorn, R.I. and Oberlander, T.M., 1982, Rock varnish: *Prog. in Phys. Geog.*, v.6, p.317-367.

Eckel, E.B., edit., 1968, Nevada test site: GSA Mem.110, 290p.

Ekren, E.B., Anderson, R.E., Rogers, C.L., and Noble, D.C., 1971, *Geology of northern Nellis Air Force Base Bombing and Gunnery Range, Nye County, Nev.*: U.S.G.S. Prof. P 651, 91 p.

Elvidge, C., 1979, *Distribution and formation of desert varnish in Arizona (MS Thesis)*: Tempe, Ariz., Arizona State Univ., 109 p.

Engel, J.L., 1980, *Thematic mapper - an interim report on anticipated performance*: Santa Barbara Research Center, 13 p.

Engel, J.L. and Weinstein, O., 1982, *The Thematic Mapper - an overview*: Insti. of Electrical and Electronics Eng., 8 p.

Engel, J.L., Lansing, J.C., Brandshaft, D.G., and Marks, B.J., 1983, *Radiometric performance of the Thematic Mapper: presentation at the seventeenth Intern. Symp. on Remote Sensing of Envir.*, Ann Arbor, Mich., May 9-13, 1983, 25 p.

Engel, C.G. and Sharp, R.P., 1958, Chemical data on desert varnish: *GSA Bull.*, v.69, p.487-518.

Farr, T.G., 1981, *Surface weathering of rocks in semiarid regions and its importance for geologic remote sensing (Ph.D. thesis)*: Seattle, Wash., Univ. of Washington, 149 p.

Farr, T.G. and Adams, J.B., 1984, Rock coatings in Hawaii: *GSA Bull.*, v.95, p.1077-1083.

Foley, D., 1978, *The geology of the Stonewall Mountain volcanic center, Nye County, Nev.*: Unpub. Ph.D. thesis,

Ohio State Univ., Columbus, Oh, 139 p.

Fontanel, A., Blanchet, C., and Lallemand, C., 1975, Enhancement of Landsat imagery by combination of multispectral classification and principal component analysis: Proceedings NASA Earth Res. Sur. Symp., July, 1975, Houston, Tex., TMX-58168, p.991-1012.

Glasby, G.P., McPherson, J.G., Kohn, B.P., Johnston, J.H., Keys, J.R., Freeman, A.G., and Tricker, M.J., 1981, desert varnish in Southern Victoria Land, Antarctica: New Zealand Jour. of Geol. and Geoph., v.24, p.389-397.

Hooke, R.LeB., Yang, H., and Weiblen, P.W., 1969, Desert varnish: an electron probe study: Jour. of Geol., v.77, p.275-288.

Hunt, C.B., 1954, Desert varnish: Science, v.120, p.183-184.

Hunt, C.B., 1961, Stratigraphy of desert varnish: U.S.G.S. Prof.P.424-B, p.194-195.

Hunt, G.R., 1977, spectral signatures of particulate minerals in the visible and near infrared: Geophysics, v.42, p.501-513.

Hunt, G.R. and Ashley, R.P., 1979, Spectra of altered rocks in the visible and near infrared: Econ. Geol., v.74, p.1613-1629.

Hunt, G.R. and Salisbury, J.W., 1970, Visible and near-infrared spectra of minerals and rocks: I. Silicate minerals: Modern Geol., v.1, p.282-300.

Hunt, G.R., Salisbury, J.W., and Lenhoff, C.J., 1973a, Visible and near infrared spectra of minerals and rocks: VI. Additional silicates: Modern Geol., v.4, p.85-106.

Hunt, G.R., Salisbury, J.W., and Lenhoff, C.J., 1973b, Visible and near infrared spectra of minerals and rocks: VII. Acidic igneous rocks: Modern Geol., v.4, p.217-224.

Hunt, G.R., Salisbury, J.W., and Lenhoff, C.J., 1973c, Visible and near infrared spectra of minerals and rocks: VIII. Intermediate igneous rocks: Modern Geol., v.4, p.237-244.

Hunt, G.R., Salisbury, J.W., and Lenhoff, C.J., 1974, Visible and near infrared spectra of minerals and rocks: IX. Basic and ultrabasic igneous rocks: Modern Geol., v.5, p.15-22.

Haydn, R., Dalke, G.W., Henkel, J., and Bare, J.E., 1982, Application of the IHS color transform to the processing of multisensor data and image enhancement: presented at the Inter. Symp. on Remote Sensing of Arid and Semi-arid Lands, Cairo, Egypt, Jan. p.599-616.

Joreskog, K.G., Klován, J.E., and Reymont, R.A., 1976, Geological factor analysis: Elsevier Scient. Pub. Co., N.Y., N.Y., 178p.

Keller, W.D., 1977, Scan electron micrographs of kaolins collected from diverse environments of origin: Clays and Clay Mineralogy, v.25, p.347-364.

Knauss, K.G. and Ku, T., 1980, Desert varnish: potential for age dating via uranium-series isotopes: Jour. of Geol., v.88, p.95-100.

Krumbein, W.E. and Jens, K., 1981, Biogenic rock varnishes of the Negev Desert (Israel): an ecological study of iron and manganese transformation by cyanobacteria and fungi: Oecologia (Berl.), v.50, p.25-38.

Laudermilk, J.D., 1931, On the origin of desert varnish: Amer. Jour. of Science, v.21, p.51-66.

Noble, D.C., 1965, Gold Flat member of the Thirsty Canyon Tuff - a pantellerite ash-flow sheet in southern Nevada: U.S.G.S. Prof. P. 525-B, p.885-890.

Noble, D.C., Anderson, R.E., Ekren, E.B., and O'Connor, J.T., 1964, Thirsty Canyon Tuff of Nye and Esmeralda Counties, Nevada: U.S.G.S. Prof.P. 475-D, p.24-27.

Noble, D.C., 1968, Kane Springs Wash volcanic center, Lincoln County, Nev: GSA Mem. 110, p.109-116.

Noble, D.C., Bath, G.D., Christiansen, R.L., and Orkild, P.P., 1968, Zonal relationships and paleomagnetism of the Spearhead and Rocket Wash members of the Thirsty Canyon Tuff, southern Nevada: U.S.G.S. Prof.P. 600-C, p.61-65.

Noble, D.C. and Christiansen, R.L., 1968, Geologic map of the southwest quarter of the Black Mountain quadrangle, Nye County, Nevada: U.S.G.S. Misc.Geol.Invest.Map I-562.

Noble, D.C. and Christiansen, R.L., 1974, Black Mountain volcanic center: in Guidebook to the geology of four Tertiary volcanic centers in central Nevada: Nev.Bur.Mines and Geol. Rept.19, p.22-26.

Noble, D.C. and Parker, D.F., 1974, Peralkaline silicic volcanic rocks of the western U.S.: Bull.Volcanology, v.38, p 803-827.

Noble, D.C., Vogel, T.A., Weiss, S.I., Erwin, J.W., McKee, E.H., and Younker, I.W., 1984, Stratigraphic relationships and source areas of ash-flow sheets of the Black Mountain and Stonewall Mountain volcanic centers, Nev.: Jour.Geoph.Res., v.89, p.8593-8602.

Novak, S.W., 1984, Eruptive history of the Kane Springs Wash volcanic center, Nevada: Jour.Geoph.Res., v.89, p.8603-8615.

Novak, S.W., 1985, Geology and geochemical evolution the Kane Springs Wash volcanic center, Lincoln County, Nevada: Unpub. Ph.D. thesis, Stanford Univ., Stanford, Calif., 173 p.

O'Connor, J.T., Anderson, R.W., and Lipman, P.W., 1966, Geologic map of the Thirsty Canyon quadrangle, Nye County, Nevada: U.S.G.S. Quad. Map GQ-524.

Perry, R.S. and Adams, J.B., 1978, Desert varnish: evidence for cyclic deposition of manganese: Nature, v.276, p.489-491.

Podwysocki, M.H., Gunther, F.J., and Blodget, H.W., 1977, Discrimination of rock and soil types by digital analysis of Landsat data: NASA Goddard Space Flight Center, X-923-77-17, 37 p.

Podwysocki, M.H., Segal, D.B., and Abrams, M.J., 1983, Use of multispectral scanner images for assessment of hydrothermal alteration in the Marysville, Utah mining area: Econ. Geol., v.78, p.675-687.

Potter, R.M. and Rossman, G.R., 1977, Desert varnish: the importance of clay minerals: Science, v.196, p.1446-1448.

Potter, R.M. and Rossman, G.R., 1979, The manganese and iron oxide mineralogy of desert varnish: Chemical Geology, v.25, p.79-94.

Rogers, C.L., Ekren, E.B., Nogle, D.C., and Weir, J.E., 1968, Geologic map of the northern half of the Black Mountain quadrangle, Nye County, Nevada: U.S.G.S. Misc. Geol. Invest. Map I-545.

Ross, C.S. and Smith, R.L., 1961, Ash flow tuffs: U.S.G.S. Prof.P.366, 81p.

Rowan, L.C., Wetlaufer, P.H., Goetz, A.F.H., Billingsley, F.C., and Steward, J.H., 1974, Discrimination of rock types and detection of hydrothermally altered areas in south-central Nevada by the use of computer-enhanced ERTS images: U.S.G.S. Prof.P. 883, 35 p.

Rowan, L.C., Goetz, A.G.H., and Ashley, R.P., 1977, Discrimination of hydrothermally altered and unaltered rocks in visible and near-infrared multispectral images: Geophysics, v.42, p.522-535.

Sabins, F.F., 1987, Remote Sensing: W.H. Freeman and Company, New York, N.Y., 449 p.

Segal, D.B., 1983, Use of Landsat multispectral scanner data for the definition of limonitic exposures in heavily vegetated areas: Econ. Geol., v.78, p.711-722.

Staley, J.T., Palmer, F., and Adams, J.B., 1982, Microcolonial fungi: common inhabitants of desert rocks: Science, v.213, p.1093-1094.

Taranik, J.V., 1978a, Characteristics of the Landsat multispectral data system: U.S.G.S. Open-file Rep. 78-187, 76 p.

Taranik, J.V., 1978b, Principles of computer processing of Landsat data for geologic applications: U.S.G.S. Open-file Rep. 78-117, 50 p.

Taranik, J.V., and Trautwein, C.M., 1977, Integration of geological remote sensing techniques in subsurface analysis: in LeRoy Ed. Subsurface Geology, Colorado School of Mines Pub., Golden, Colo., p.767-787.

Trautwein, C.M. and Taranik, J.V., 1978, Analytical and interpretive procedures for remote sensing data: U.S.G.S. Open-file Rep. 78- , 52 p.

Tschanz, C.M. and Pampeyan, E.H., 1970, Geology and mineral deposits of Lincoln County, Nev.: Nev.Bur.Mines and Geol. Bull. 73, 188 p.

Weiss, S.I., 1985, Stratigraphy and paleomagnetic studies of ash-flow tuffs of the Black Mountain and Stonewall Mountain volcanic centers: Unpub. MS thesis, University of Nevada, Reno, Nev.

White, C.H., 1924, Desert varnish: Amer.Jour.Sci., v.7, 5th ser., p.413-420.